ANTIGENIC AND MOLECULAR CHARACTERIZATION OF AVIAN REOVIRUSES

by

OLATUNDE GBOLAHAN OLUWAYINKA

(Under the Direction of Holly S. Sellers)

ABSTRACT

Avian reovirus (ARV) infections are an important cause of economic losses in commercial poultry worldwide, including the United States. Since 2011, increased cases of ARV-associated tenosynovitis in the progeny of vaccinated breeder flocks have raised concerns about the declining efficacy of existing vaccines. This is compounded by limitations in current virus characterization schemes, which offer little insight into key pathobiological traits such as virulence, tissue tropism, and lesion type. These limitations hinder our ability to distinguish pathogenic strains from commensals, especially given ARV's ubiquity in poultry environments.

A further challenge in ARV characterization is the frequent presence of multiple co-infecting strains in clinical samples. Accurate identification of these strains is essential for outbreak tracking and evaluating control strategies.

To address these challenges, we conducted three complementary studies. First, we assessed antigenic relatedness among ARV field isolates through cross-neutralization assays involving 10 field strains and their respective antisera, representing all seven known genotypic clusters (GCs). Second, we evaluated the Oxford Nanopore Technologies MinION platform for its ability to

resolve mixed ARV populations in clinical samples. Third, we sequenced the complete genomes of 12 field isolates and performed phylogenetic analyses using amino acid sequences from individual proteins and the full viral proteome.

Our findings show that ARV antigenic diversity is broader than previously recognized, with all seven GCs and three sub-clusters tested in these studies representing distinct serotypes. Third-generation sequencing provided deeper resolution of ARV subpopulations compared to conventional methods. Predicted whole proteome phylogeny was largely congruent with the current σC-based classification suggesting σC evolution reflects whole virus evolution. In addition, we report the first full genome sequences of GC7 isolates, offering new insights into the genetic makeup of this understudied cluster.

INDEX WORDS: Avian reoviruses, Serotypes. Molecular Characterization, Serological relatedness, Minion amplicon sequencing, Whole genome sequencing, Phylogenetic analysis, Next generation sequencing

ANTIGENIC AND MOLECULAR CHARACTERIZATION OF AVIAN REOVIRUSES

by

OLATUNDE GBOLAHAN OLUWAYINKA

DVM, Federal University of Agriculture Abeokuta, Nigeria, 2009

MSc., University of Ibadan, Nigeria, 2014

A Dissertation Submitted to the Graduate Faculty of the University of Georgia

in Partial Fulfillment of the Requirements for the Degree

DOCTOR OF PHILOSOPHY

ATHENS, GEORGIA

2025

ANTIGENIC AND MOLECULAR CHARACTERIZATION OF AVIAN REOVIRUSES

by

OLATUNDE GBOLAHAN OLUWAYINKA

Major Professor: Holly S. Sellers

Committee: Maricarmen Garcia

James Stanton

Steven Conrad

Electronic Version Approved:

Ron Walcott

Vice Provost for Graduate Education and Dean of the Graduate School

The University of Georgia

May 2025

DEDICATION

I would like to dedicate this dissertation to God, my family and friends who supported me with unwavering love.

ACKNOWLEDGEMENT

I would like to express my sincere appreciation to Dr. Holly S. Sellers for your continuous support, guidance and profound contribution to my professional and personal growth. I was also honored to have Dr. Steve Conrad and Dr. James Stanton and Dr. Garcia Maricarmen on my committee. I am truly grateful for their advice, guidance and support.

Finally, I am indebted to the faculty, staff, and students at the Poultry Diagnostic and Research Center, College of Veterinary Medicine (Dr. Stanton's laboratory), and the staff of Conrad's laboratory at the US National Poultry Research Center (Dr. Conrad's laboratory) who have aided me in every aspect of completing this work; in particular, I would like to acknowledge Drs. Alvarez-Narvaez and Harrel.

Further, I would like to acknowledge the past and present staff of the PDRC Virology laboratory for their help and support through the course of this project these projects, specifically: Erich Linneman, Vanessas Gauthiersloan, Nicholas Davis-Fields Amanda Greenway.

TABLE OF CONTENTS

Page

LIST OF TABLES

LIST OF FIGURES

CHAPTER 1

INTRODUCTION AND LITERATURE REVIEW

Avian reovirus – Taxonomy

Avian reovirus is a member of the *Reoviridae* family, the largest of the dsRNA viruses. It is divided into two subfamilies: *Spinareovirinae* and *Sedovirinae*. The member genera in this family include *Orthoreovirus, Rotavirus, Orbivirus* and others. ARV and the mammalian reoviruses are classified within subfamily *Spinareoevirinae* and make up the bulk of the genus *Orthoreovirus* (1). The subfamily *Sedovirinae* to which rotavirus belongs are characterized by the absence of large surface projections which are prominent on the *Spinovirinae* (2).

Enteritis is often the clinical outcome of rotavirus infection in poultry, particularly in turkey poults (3). The ARVs are ubiquitous in poultry environments and mostly non-virulent, making it difficult to infer causality when isolated from lesions. However, the virus has been identified as the definitive cause viral arthritis and tenosynovitis in commercial poultry (4).

Avian Reovirus Disease

ARV is ubiquitous in poultry environments, and due to its nonenveloped structure, it can persist in the environment for extended periods. Viral arthritis/tenosynovitis, runting stunting syndrome, enteritis, hepatitis and malabsorption syndrome are some of the pathologies induced by ARV infections in susceptible chicken and turkey flocks (4, 5). Of these, ARV has been identified as the definitive cause of viral arthritis/tenosynovitis (6-8). Clinical signs in affected birds include

lameness, swollen hocks and tendons and possible rupture of gastrocnemius and digital flexor tendons may occur in heavier birds. Younger birds have been reported to be more susceptible to development of clinical disease (9). Localized replication of the virus in the tendons and synovial membrane of the hock has been established (10). Infiltration of mononuclear cells in these areas results in pathological changes including cartilage erosion and thickening of the tendons due to fibrosis (11). Recently, the severity of ARV induced tenosynovitis has been linked to increased percentage IFN-γ expressing $CD8^+$ cells in infiltrating mononuclear cells (8)

In malabsorption syndrome (MAS), the role of ARV is uncertain with reports suggesting it is a primary etiology with some strains inducing marked enteritis and poor growth performance (9) while others indicate that its contribution is secondary (12). However, under experimental conditions 'MAS strains' of ARV have been reported to induce signs consistent with MAS including abnormal feathering patterns, depigmentation of beaks and shanks, pale mucous membranes, lameness, diarrhea and undigested feed particles in droppings (13). In addition, torticollis and tremor and other central nervous system signs have been associated with enteric ARV (14, 15).

Diagnosis of Viral Arthritis

Clinical presentation is often sufficient for initial diagnosis of viral arthritis. However, owing to the presence of other poultry pathogens that present similarly, an holistic approach must be taken in gathering the relevant flock details such as: clinical signs, lesions, mortality patterns, production parameters, vaccinations and other records of flock history (16). These may be followed by diagnostic confirmation wherein virus isolation from tendons, joints and/or synovial fluid of affected chickens is the gold standard (17). ARV can be cultured in specific pathogen free (SPF) embryos and primary tissue cultures prepared from them: chicken embryo liver cells

(CELiC), and chicken embryo kidney cells (CEK) (18, 19). In addition, Leghorn male hepatocellular cell lines (LMH) support the growth of field isolates of ARV, and are widely employed in laboratories for this purpose (20).

RT-PCR amplification and Sanger sequencing of a portion of the viral S1 segment coding for Sigma C (minor outer capsid protein) is routinely done for molecular characterization of ARV (21, 22). The predicted amino acid sequence of this protein is employed in phylogenetic clustering of the virus. Based on this typing scheme seven genetic clusters and several subclusters within them have been described (23).

Avian Reovirus Genomic Structure

Avian reovirus is a pathogen of concern in poultry producing areas of the world, either directly or in association with other pathogens causes economically impactful diseases in various avian species (4). The genus *Orthoreovirus* to which ARV belongs also comprises other well characterized mammalian reoviruses (MRV) and together they make up the bulk of viruses in this genus. Avian reoviruses are non-enveloped viruses with an external diameter of 75nm. ARV virions possess an icosahedral capsid which is made up of two concentric protein shells and encompasses a genome composed of 10 segments of double stranded RNA. The genomic segments are named based on their electrophoretic mobility, viz: large (L1-L3), medium (M1-M3) and small (S1-S4). This genome encodes 8 structural proteins (λA, λB, λC, μA, μB, σA, σB, and σC,) and 4 nonstructural proteins (μNS, σNS, p10 and p17) (24).

L1 Segment

L1 is 3879 nucleotides long and encodes the major core protein, λA which is made up of 1293 amino acid residues (25). This protein is a major component of the inner core shell, which covers the viral genome and viral RNA polymerase. λA when transfected into cells individually

was dispersed in the cytoplasm, but when associated with μNS, it is rapidly incorporated into viral factories (24).

The predicted amino acid sequence of λA contains a conserved hydrophilic region (residues 1-110) within which is co-located with a variable region (residues 19-51), and a C_2H_2 zinc-binding motif is located at residues 182-202 (25).

Phylogenetic analysis of λA encoding gene reveals divergence into three lineages and there is no correlation between viral serotypes based upon sigma C or pathotypes and the lineages (25).

L2 Segment

The ARV L2 segment is 3830 nucleotide sequences long and encodes for the minor core protein λB which consists of 1259 amino acid residues (26). Prior to its sequencing it had been identified as the RNA dependent RNA polymerase (RdRp) based on specific properties it shares with other viral RNA polymerases (24). Following its sequencing, comparative analysis with the mammalian reovirus (MRV) L2 gene showed that there is 55% amino acid identity between ARV λB and MRV λ3 protein, thus making it the most highly conserved of known *Orthoreovirus* proteins. In addition, a predictive structure/function analysis of ARV λB carried out by mapping to MRV λ3 showed that most of the identical amino acids and conservative substitutions were located near and within catalytic domains and lining RdRp channels (26). These findings strongly suggest minimal evolutionary divergence in areas predicted to contain the polymerase motif and residues that interact with template in RdRp proteins, which preserves their function (26).

L3 Segment

The L3 segment is 3855 nucleotides long and encodes λC, made up of 1285 amino acid residues (25). λC is the viral mRNA capping enzyme and extends from the inner core to the outer

capsid of ARV (24). This protein, occurring as homopentamers, forms the turrets projecting from the five-fold axes of ARV cores (27).

At positions 169 and 188, λC shows the presence of two conserved K residues indicative of guanylyl transferase activity. It also possesses an ATP/GTP-binding site motif A (residues 379-386) and a conserved S-adenosyl-L-methionine-binding motif suggestive of methylase activity at residues 822-830 (25).

M1 Segment

The M1 segment is 2283 base pairs long and encodes the minor core protein μA, which consists of 732 amino acid residues (28). μA possesses NTPase and RTPase activity similar to its functional analogue in MRV, μ2. These functional properties of μA suggest that it might be important for generating energy for viral RNA synthesis. However, the importance of μA to this integral viral process might not be significant since the ARV structural protein σA also has NTPase and RTPase activities, and the probability that other ARV proteins have similar properties is high considering that MRV viral protein λ1 also shows same activities.

M2 Segment

The ARV M2 segment is 2158 base pairs long and encodes the major capsid protein μB which consists of 676 amino acids residue (28). M2 viral segment might contribute significantly to the evolution of ARV strains. As was observed in an earlier study when isolates were grouped according to virulence, M2 was found to be second most variable segment, next to S1 (29). Similarly, compared to other ARV M-class segments M2 was reported to be the most divergent (28). This finding was supported by Egana-Labrin et al., (30) who found that, after S1 segment, M2 was more divergent than other ARV genome segments. Also, a recent study in mammalian reovirus provided evidence to suggest that M2 gene was a determinant of MRV induced

myocarditis (31). However, recently it was reported that M3 was the most divergent of the M-class segments and second most divergent of all ARV segments (32).

The majority of μB produced during ARV infection is cleaved. The cleavage products of μB are: μBN, a myristoylated amino-terminal peptide, and μBC, a large carboxy terminal protein (24). μB, μBN and μBC are components of ARV outer capsid (33). μBC is particularly important for release of transcriptionally active ARV core into cytoplasm. Following intra-lysosomal uncoating, μBC undergoes two sequential cleavages at a site close to its C-terminus to produce δ and δ^1 polypeptides. These cleavages are necessary to promote interaction with lysosomal membranes and conformational changes, which are necessary steps for the release of viral cores (24).

M3 Segment

The M3 segment is 1996 base pairs long and encodes for the nonstructural protein μNS which consists of 635 amino acid residues (28). Based on inter-genotypic cluster comparison, in contrast to intra-genotypic cluster comparison reported by other studies (28, 30), M3 was found to be most divergent of the ARV M-class segments and the second most divergent after S1 (32). It has been predicted from the deduced amino acid sequence of μNS that it contains two coiled coil segments between positions 451-472 and 540-599 which are separated by a short stretch of amino acid residues (34). This finding and the observation that removal of the first coil from MRV μNS (nonstructural protein encoded by MRV M3 segment) resulted in loss of function which was rescued by the replacement with green fluorescent protein (GFP), a protein known to dimerize, suggest that μNS form oligomers possibly facilitated by interaction domains on the first coil (35). Later, evidence was provided that μNS monomers self-associate to form homo-oligomers and that the C-terminal domain was important for this process (36).

μNS is the only ARV protein capable of forming inclusions when expressed in the absence of any other viral protein and the inclusion formed in μNS transfected cells are similar in appearance to those found in ARV infected cells (34). Therefore, μNS appears to be the minimal requirement for the formation of viral factories in ARV infected cells. Further, co-transfection of μNS with other viral proteins suggests that it selectively recruits σNS and λA into viral inclusions (37). An experiment using truncated μNS found that the region between μNS residues 448 to 635 was the smallest protein length required for inclusion formation while amino acid residues from 140-380 were shown to be involved in inclusion maturation (36).

While both ARV and MRV form cytoplasmic viral factories, they differ in the nature and morphogenesis of the viral factories they form. The MRV form filamentous, microtubule associated inclusions, whereas, those of ARV are globular, non-filamentous and non-microtubule associated (34, 38).

μNS-formed inclusions have found utility in protein purification and validation of protein-protein interactions inside the cytoplasm or nucleus of living cells (9). Recently, these inclusions have been tested as vectors in subunit vaccines (39, 40).

S1Segment

The S1 segment of avian *Orthoreovirus* is functionally tricistronic (41). This segment encodes three partially overlapping ORFs and codes for one structural (σC) and two non-structural proteins (p10 and p17).

P10 Protein

ORF1 of avian reovirus genomic segment S1 is expressed as 10 kDa transmembrane type 1 protein. This protein has been found to be responsible for the fusogenic phenotype which results in the characteristic syncytium displayed by avian reovirus infected cells (41). In contrast, MRVs

are typically not fusogenic except for Nelson Bay virus and baboon reovirus (42). P10 is described as fusion-associated small transmembrane (FAST). It possesses a central transmembrane domain that separates the ectodomain from the endodomain (42). p10 is expressed in virus infected cells and its insertion into the membrane of host cell results in membrane destabilization which has been associated with faster viral egress (43).

However, aside from the fact that it is atypical of non-enveloped viruses to contain a fusion protein, the ARV p10 is also uncharacteristically secreted in its active form and since membrane fusion is a late process in viral replication it is therefore important to understand the mechanisms by which ARV p10 remains inactive until viral egress. A previous study demonstrated that the p10 ectodomain targets the protein for rapid degradation when inserted early into host cell membrane (44). A recent study (45) identified E3 ubiquitin ligase - seven in absentia homolog 1 (SIAH-1) in association with lysosome-associated membrane protein 1 (LAMP-1) as the specific host factors that drive rapid degradation of ARV p10. Therefore, a combination of viral and host mechanisms ensures rapid degradation of p10. Since there is no temporal regulation in the production of p10 in comparison to other membrane fusion proteins, it is thought that this rapid degradation in the early stages of viral infection prevents the trafficking of p10 to the cell membrane, but at later stages of viral replication the p10 degradation mechanism appears overwhelmed leading to the eventual insertion of p10 into the host cell plasma membrane (44).

p17 Protein

ORF 2 of the ARV S1 segment codes for the 17 kDa protein called p17. It is a unique viral protein with no known homology to any other protein (24). Although no particular function has been attributed to this protein in ARV life cycle, more recent studies have been able to shed light on its effect in infected cells. p17 is a nucleocytoplasmic shuttling protein which has been reported

to trigger several signaling pathways leading to the induction of autophagy (46). The nucleocytoplasmic shuttling of p17 is dependent upon its interaction with the host protein heterogenous nuclear ribonucleoprotein (hnRNP) A1 and lamin A/C. Specific regions of the p17 protein that interact with these host proteins have been identified (47). Furthermore, p17 has also been reported to possess a cell growth retardation function through activation of p53 and cyclin-dependent kinase (CDK) inhibitor (48). In addition, the p17 has been reported to possess an anti-angiogenic effect.

Sigma C protein

σC is a minor outer capsid protein responsible for cell attachment (49). The σC protein consists 326 amino residues and it is encoded by the third open reading frame of the S1 viral genomic segment. This protein, similar to its mammalian counterpart σ1, is multimeric and is present in subviral particles but not viral cores and is relatively resistant to proteolytic digestion (49).

The homotrimeric σC protein forms the fibrous cell attachment protein of ARV (50). It is made up of the amino terminal tail consisting of 1-50 amino acid residues, stalk (51-156 residues) and the carboxy terminal head domain (156-326 amino acid residues) responsible for receptor binding (51)

Neutralizing antibodies against σC are elicited during ARV infection and it has been shown that these antibodies are able to prevent infection from homologous challenge (49, 52). The σC neutralizing antibodies elicited are strain specific (53). Also, this ARV surface protein is a potent inducer of apoptosis (54) and injection of recombinant σC into virus-induced fibrosarcoma leads to tumor regression (55). Several mechanisms have been found that contribute to ARV σC mediated apoptosis including: DNA damage resulting in upregulation of some DNA damage-

responsive genes (56); exploitation of the p53 dependent pathway of apoptosis (57); and the eukaryotic elongation factor 1 alpha 1 (EEF1A1) has been identified as the pro-apoptotic host factor that partners with ARV σC which results in apoptosis of tumor cells(58)

Among the ARV proteins, σC is the most variable contributing immensely to the genetic diversity observed among strains. Partial or complete sequences of the ARV σC have been used for genetic characterization of ARV isolates (21). Presently, seven genotypic clusters have been reported for ARV based on σC sequences.

S2 Segment

The S2 segment encodes the ARV structural protein σA, which is a component of the ARV inner core (24). In infected avian cells, ARV sigma A protein has been found to be colocalized with μNS in cytoplasmic viral factories, and to a limited extent they have been found localized in the nucleoplasm (59). The sigma A protein has been shown to be important for ARV replication and evasion of innate immune response.

An earlier study had found that the σA protein is important for binding the λA protein building blocks of the inner viral core thereby supplying rigidity and ensuring that the core is rendered impenetrable to more viral nucleic acid molecules (60). In this study, infection with a temperature sensitive mutant with an amino acid change of proline to leucine at amino acid position 158 of the σA protein was found to produce approximately 100-fold fewer particles at the non-permissive temperature compared to the permissive temperature. The authors suggested that this change may have resulted in the inability of the outer capsid protein σC to condense onto nascent cores. More recently, a study aimed at identifying host factors that stabilize viral proteins during replication found that the T-complex protein-1 ring complex (TRiC), a eukaryotic chaperone protein, stabilizes σA, σC and σNS viral proteins by preventing their degradation by the

ubiquitin-proteasome pathway. In addition, knockdown of TRiC subunits and the consequent reduction in expression levels of σA protein and other TRiC-chaperoned viral proteins resulted in more than a twofold diminishment in ARV titer when compared to controls (61).

On the other hand, σA binds dsRNA in sequence-independent manner making it a functional analogue of mammalian reovirus σ3 protein. The capability of σA to bind dsRNA inhibits the activation of IFN induced, dsRNA-dependent PKR and 2'-5 -oligoadenylate synthase antiviral pathways possibly contributing to the ability of ARV to resist the IFN-induced antiviral state (62). Also, σA protein has been identified as an activator of the P13/Akt pathway – an intercellular signaling pathway in cellular processes such as cell proliferation, differentiation and survival (63).

S3 Segment

The ARV σB protein is encoded by the 1196 bp S3 segment of the genome. The S3 segment is monocistronic with an ORF that possesses the AUG initiation codon at residue 24 and extends for 367 codons (64). The σB protein is a major protein of outer capsid of ARV which similar to σC induces neutralizing antibodies; however, unlike σC the antibody induced is group specific (65). Therefore, σB is of interest in serological diagnosis of ARV infections (66-68). A deeper analysis of the antibody response to σB protein found two highly reactive linear epitopes which were shown to be conserved among ARV strains examined in this study (69)

Also, there is evidence that σB is important in the pathogenesis of ARV induced arthritis. An *in vitro* study which employed DNA arrays to identify differentially expressed genes (DEGs) following transfection of CEFs with recombinant σB, found that σB upregulated genes associated with the arthritis pathway and downregulated some others that are important for maintaining articular integrity (70).

S4 Segment

σNS is a nonstructural protein and the translational product of S4 segment of ARV genome. This protein binds ssRNA in a sequence independent manner and it is recruited into inclusion bodies by another nonstructural protein, μNS (71-73). The dispersion of RNA binding domains along the length of σNS is indicative of a conformational interaction with RNA molecules and, coupled with its rapid and early inclusion into viral factories, (72) led earlier researchers to suggest that σNS might be important for replication and packaging of viral RNA. Recently, several studies have provided evidence of the role of σNS in these important viral processes. Boredavka et al (2015) showed that the active RNA binding form of σNS is a hexamer with the ability to bind to nucleic acid molecules, which initiates ATP-dependent helix unwinding of bound RNA, a phenomenon common to RNA chaperones. Aside providing evidence that σNS is an RNA chaperone ensuring proper folding of viral RNA, the investigators further showed that when a hexamer of σNS binds to two ssRNA molecules with base complementarity there is rapid strand annealing, thus facilitating specific and stable RNA-RNA interactions between genome segment precursors. In addition , a study with MRV provided evidence that viral mRNAs are only recruited into viral factories when σNS is present and able to bind RNA, suggesting that σNS is indispensable for viral replication (74).

Epidemiology of ARV

Fahey and Crawley (1952) isolated a virus in birds suffering from a chronic respiratory disease in 1952 (75). While studying *Mycoplasma synoviae*, Olson, and Kerr, (76) isolated synovitis-inducing organisms from lesions of broilers which was later found to be a virus and dubbed 'viral arthritis agent'. In 1972 both viral arthritis agent and Fahey-Crawley virus were found to induce similar gross and histologic lesions in broilers (6). An electron microscopy study

of the viral arthritis agent provided conclusive evidence that this agent was reovirus (6). In the years following, several other strains of ARV causing tenosynovitis in chickens were isolated in the U.S., notably, the s1133 strain, which will later become the cornerstone of ARV control in commercial poultry flocks across North America following its attenuation in the 1970s (17). S1133 was isolated by Drs. Van der Heide, L, Geissler, J and Bryant, E (11).

Earlier studies on the molecular characterization of ARV field isolates suggested that isolates from the United States were less divergent, with most of U.S. isolates clustering with common vaccine strains, while isolates from the Netherlands, Germany and Taiwan were more divergent (21, 77, 78). However, in 2012 a trend of increased variant isolation from field cases of viral tenosynovitis was observed in the U.S. (17). Variant isolation has also been reported from other countries including: Brazil (79), Israel (80), China (81-83), Canada (78, 84), Iran (85, 86), and France (87).

ARV Vaccines

Live Modified and Inactivated Vaccines

The combination of live and inactivated vaccines in a prime-boost strategy has been identified as one of the most effective approaches for inducing protective immunity against ARV disease in chickens (88). Chicks are more susceptible to ARV infection and manifestation of clinical signs, therefore vaccines are administered to breeder hens to ensure transfer of passive immunity to progenies, though early vaccination of chicks with live vaccine is sometimes practiced (4). S1133 and other GC 1 strains, including 1733, 2408 and Miss B, have historically been used in commercial live vaccine preparation against ARV. However, reports of variant infection in the presence of antibodies induced by these vaccines have cast doubt on their efficacy. A more recent commercial live vaccine preparation departed from the trend of including GC 1 strains and is

composed of antigenic variant reovirus serotypes 1/4455, 2/4455, and 3. Generally, the level of antibodies induced by immunizations with live ARV vaccines are higher and long lived compared to antibody immunity generated by inactivated vaccines. Unfortunately, the emergence of variants hampers the efficacy of both commercial live and inactivated vaccines. Nevertheless, vaccination protocols that include 2 to 4 immunizations with commercial live vaccines followed by inactivated preparations have been found to be more effective.

In 1975, an S1133 derived inactivated vaccine was tested in broiler breeders to determine their effectiveness in passive transfer of protective immunity to their progeny. Results showed that antibody response was low and short lived (89). Inactivated autogenous ARV vaccines made from circulating strains within a production complex or region have grown in use within the US poultry industry owing to the lack of efficacious commercial vaccines. The process of determining the strain to include in an autogenous vaccine requires diligent and thorough sampling, strain characterization in breeder and broiler flocks and in vivo pathogenicity studies of isolated strains when necessary (17).

Internationally, commercial vaccines (based on GC 1 strains) are also used and the emergence of infections by variant strains in the presence of immunity generated by these vaccines appears to be common experience (87, 90-93). In Israel, a novel approach has been introduced to control the circulation of immune escape variants. Using a controlled exposure approach as described by Perelman, B, Krispin, H, Solomon, A, Elrom, K and Farnoushi, Y (94) – breeder flocks vaccinated with an inactivated vaccine at 5 -7 weeks of age are vaccinated again at 10 weeks with a live hot strain of the circulating ARV followed by another inactivated vaccine at 18 – 20 weeks. As of 2022, the incidence of ARV GC 5 infections, the cluster to which most pathogenic strains in Israel belong, has been significantly reduced in both breeders and broilers. In the latter

population, it was reported that prior to implementation of this regimen of vaccination, large losses were recorded due to slaughterhouse condemnations owing to stricter than usual meat quality regulations stipulated by Kosher dietary laws (95).

Recombinant Reovirus Vaccines

Recombinant reovirus vaccines have been explored for protection of turkeys against reovirus induced arthritis. Owing to the absence of a commercial vaccines for turkey reoviruses autogenous vaccines are increasingly common; however, they are hampered by the lack of life prime. A promising approach involves using live virus vectors such as *Pichinde virus* (PiV) to deliver ARV antigens. Studies have shown that a PiV-vectored recombinant vaccine expressing ARV proteins and administered orally can effectively reduce viral loads in multiple tissues (96). A similar approach has been evaluated for the control of reovirus induced hemorrhagic disease in grass carp. *Lactococus lacti* was engineered to express the capsid protein of grass carp reovirus and administered orally (97). The authors reported that this vaccine was able to increase the survival rate in a challenge experiment with virulent grass carp reovirus strains. Both recombinant vector vaccines (PiV and *L.lacti)* have been shown to induce strong humoral and cell mediated immune responses (98, 99). Aside their immunological value, these vectors are safe. PiV is native to rice rats in the Pichinde Valley of Colombia, and antibodies to this virus are not prevalent in most farm animals, while *L. lactis* is a commensal of the gut. Therefore, both vectors are able to persist in the gut for extended periods thus facilitating the development of robust immunity against expressed recombinant antigens. However, there is dearth of studies evaluating the use of these vectors in poultry, although they could be promising vaccine vectors for poultry pathogens.

Reovirus Subunit Vaccines

Due to the continued emergence of field variants of ARV with the ability to evade immunity induced by existing vaccines the need for new ARV vaccine is critical (17). However, the high cost associated with developing and licensing new live and attenuated vaccines, coupled with their potential to become rapidly ineffective due to viral evolution, has made subunit vaccines an attractive alternative. Subunit vaccines are relatively easier to produce and offer the advantage of being amenable to rapid updates should immune escape mutants emerge (53).

Among ARV proteins, σC has been the primary focus for subunit vaccine development due to its status as the immunodominant viral protein and its ability to induce type-specific neutralizing antibodies. Goldenberg, D, Lublin, A, Rosenbluth, E, Heller, ED and Pitcovski, JJV (53) reported that a truncated σC protein consisting of the globular head, stalk and hinge region induced significantly greater antibody response compared to full length protein. An earlier study showed that full-length σC protein displayed on *Enterococcus faecium*, a lactic acid bacterium, induced a robust immune response (100). Additionally, subunit vaccines incorporating ARV σC and σB displayed on the baculovirus envelope have been evaluated (66). In this study, serum derived from mice immunized with individual recombinant viral protein subunits or in combinations revealed that σC induced a greater number of neutralizing antibodies compared to σB; however, the titer when both subunits were jointly administered was several folds higher than titer produced when used singly (66). Results of this study suggest that σB, though less immunogenic, might also be a promising viral subunit. Vaccines were not adjuvanted in this experiment but were delivered intraperitoneal.

In addition, ARV σC-based subunit vaccines have been expressed on novel platforms including yeast (101). Recombinant σC produced in yeast was found to be less susceptible to

degradation in the intestine and induced a strong immune response when added to feed at high dose (250 μg) (101). Plants, with hardier cell walls and capacity for large scale production of recombinant subunit proteins have been investigated for the production of σC-based subunit vaccines (102-104). However, most attempts at plant-made σC subunit vaccines have resulted in a low yield of the protein despite extensive codon optimization and subcellular targeting of σC protein to chloroplasts (104). In one experiment in which σC protein was expressed in *Arabidopsis*, SPF chickens fed or subcutaneously injected the plant-expressed σC protein at weekly interval for 3 consecutive weeks, showed 70% and 90% protection, respectively (105).

In other species, σC-based subunit vaccines have been evaluated for the control of virulent reovirus. In ducks, novel duck reovirus (NDR) as gained heightened importance in China since early 2000s due to its ability to infect a wider range of duck species and higher pathogenicity compared to other duck reoviruses (106-108). A subunit vaccine based on recombinant full length NDR σC inserted in baculovirus and expressed in Sf9 cells has been tested (109). Following 2 doses of recombinant σC with Freud's adjuvant, the σC based subunit vaccines group developed high σC specific neutralizing titer, high humoral and cell mediated immune (CMI) response and 100% protection in chicks challenged with the live whole NDR. The similarly adjuvanted and dosed inactivated vaccine group showed comparable results to subunit recipients, except it was less protective (80%) in duck embryos (109). In this experiment, a live vaccine prime was not used, though live NDR vaccines are able to stimulate protective immunity against virulent NDR in ducks (110). Therefore, a possibility is that in the presence of live prime, the efficacy of the activated vaccine might be better than that of the subunit.

The σC of Muscovy duck reovirus (MDR) has also been explored as a subunit vaccine both alone and in combination with σB (111). The authors reported that there was no significant

difference in performance of both subunit vaccines. Interestingly, in one of the experiments in the study it was found that the protective response elicited by the σC-based subunit against tenosynovitis developed more rapidly compared to the divalent subunit, though the later induced a more robust protection when fully developed. It was concluded that the MDR σB might not be an efficient immunogen and that it was possible that it dampened response to σC since an earlier experiment had reported the inability of a σB subunit vaccine to induce detectable antibodies in vaccinated ducks (112). In both studies the adjuvant used was not identified but was referred to as "a water-in-oil adjuvant routinely used for inactivated avian vaccines". The quality of adjuvant is critical for induction of effective immune response by more conserved immunologically subdominant antigens such as σB (113).

Finally, in all of the studies on subunit vaccines for ARV, to the best of the authors' knowledge, none attempted cross neutralization experiments with strains of ARV other those bearing cognate proteins to the subunits being tested. As such, these experiments did not address the major disadvantage of subunit vaccines: the elicitation of a narrow immune response.

References

1. Andrew M.Q. King MJA, Eric B. Carstens, Elliot J. Lefkowitz. Family - Reoviridae. In: King AMQ, Adams MJ, Carstens EB. Lefkowitz EJ, editors. *Virus Taxonomy*. San Diego: Elsevier. p. 541-637; 2012.

2. Walker PJ, Siddell SG, Lefkowitz EJ, Mushegian AR, Adriaenssens EM, Dempsey DM, Dutilh BE, Harrach B, Harrison RL, Hendrickson RC*, et al.* Changes to virus taxonomy and the Statutes ratified by the International Committee on Taxonomy of Viruses (2020). *Archives of Virology.* 165:2737-2748; 2020.

3. Spackman E, Day JM, Pantin-Jackwood MJ. Astrovirus, reovirus, and rotavirus concomitant infection causes decreased weight gain in broad-breasted white poults. *Avian Diseases.* 54:16-21; 2010.

4. Jones RC. Avian reovirus infections. *Rev Sci Tech (International Office of Epizootics).* 19:614-625; 2000.

5. Egana-Labrin S, Jerry C, Roh HJ, da Silva AP, Corsiglia C, Crossley B, Rejmanek D, Gallardo RA. Avian reoviruses of the same genotype induce different pathology in chickens. *Avian Diseases.* 65:530-540; 2021.

6. Walker ER, Friedman M, Olson N. Electron microscopic study of an avian reovirus that causes arthritis. *Journal of ultrastructure research.* 41:67-79; 1972.

7. Ngunjiri JM, Ghorbani A, Jang H, Waliullah S, Elaish M, Abundo MC, Mahesh KC, Taylor KJ, Porter RE, Lee CW. Specific-pathogen-free turkey model for reoviral arthritis. *Vet Microbiol.* 235:170-179; 2019.

8. Ayalew LE, Ahmed KA, Popowich S, Lockerbie BC, Gupta A, Tikoo SK, Ojkic D, Gomis S. Virulence of emerging arthrotropic avian reoviruses correlates with their ability to activate and

traffic interferon-gamma producing cytotoxic CD8(+) T cells into gastrocnemius tendon. *Front Microbiol.* 13:869164; 2022.

9. Roessler D, Rosenberger JJAd. In vitro and in vivo characterization of avian reoviruses. III. Host factors affecting virulence and persistence. 555-565; 1989.

10. Jones RC, Islam MR, Kelly DF. Early pathogenesis of experimental reovirus infection in chickens. *Avian Pathol.* 18:239-53; 1989.

11. Van der Heide L, Geissler J, Bryant E. Infectious tenosynovitis: serologic and histopathologic response after experimental infection with a Connecticut isolate. *Avian diseases.*289-296; 1974.

12. Montgomery RD, Boyle CR, Maslin WR, Magee DL. Attempts to reproduce a runting/stunting-type syndrome using infectious agents isolated from affected Mississippi broilers. *Avian Diseases.*80-92; 1997.

13. Awandkar SP, Moregaonkar SD, Manwar SJ, Kamdi BP, Kulkarni MB. Comparative investigations of infectious runting and stunting syndrome in vaccinated breeder chicks by inactivated reovirus and chicks from non-vaccinated breeders. *Iran J Vet Res.* 18:6-12; 2017.

14. Van de Zande S, Kuhn E-M. Central nervous system signs in chickens caused by a new avian reovirus strain: a pathogenesis study. *Vet Microbiol.* 120:42-49; 2007.

15. Dandár E, Bálint Á, Kecskeméti S, Szentpáli-Gavallér K, Kisfali P, Melegh B, Farkas SL, Bányai K. Detection and characterization of a divergent avian reovirus strain from a broiler chicken with central nervous system disease. *Archives of virology.* 158:2583-2588; 2013.

16. Gamble T, Sellers H. Field control of avian reoviruses in commercial broiler production. *Avian Diseases.* 66:427-431; 2022.

17. Sellers HS. Current limitations in control of viral arthritis and tenosynovitis caused by avian reoviruses in commercial poultry. *Vet Microbiol.* 206:152-156; 2017.

18. Guneratne J, Jones R, Georgiou K. Some observations on the isolation and cultivation of avian reoviruses. *Avian Pathology.* 11:453-462; 1982.

19. Rosenberger JK, Olsen N, Van der Heide L. Viral arthritis/Tenosynovitis and other reovirus infections. *A laboratory manual for the isolation and identification of avian pathogens.* 4:207-210; 1998.

20. Kawaguchi T, Nomura K, Hirayama Y, Kitagawa T. Establishment and characterization of a chicken hepatocellular carcinoma cell line, LMH. *Cancer research.* 47:4460-4464; 1987.

21. Kant A, Balk F, Born L, Van Roozelaar D, Heijmans J, Gielkens A, Ter Huurne A. Classification of Dutch and German avian reoviruses by sequencing the sigma-C protein. *Veterinary research.* 34:203-212; 2003.

22. Liu HJ, Lee LH, Hsu HW, Kuo LC, Liao MH. Molecular evolution of avian reovirus. *Virology.* 314:336-349; 2003.

23. Sellers HS. Avian reoviruses from clinical cases of tenosynovitis: An overview of diagnostic approaches and 10-year review of isolations and genetic characterization. *Avian Diseases.* 66:420-426; 2022.

24. Benavente J, Martínez-Costas J. Avian reovirus: structure and biology. *Virus research.* 123:105-119; 2007.

25. Shen PC, Chiou YF, Liu HJ, Song CH, Su YP, Lee LHJRivs. Genetic variation of the λA and λC protein encoding genes of avian reoviruses. 83:394-402; 2007.

26. Xu W, Coombs KMJVj. Avian reovirus L2 genome segment sequences and predicted structure/function of the encoded RNA-dependent RNA polymerase protein. 5:1-11; 2008.

27. Zhang X, Tang J, Walker SB, O'Hara D, Nibert ML, Duncan R, Baker TS. Structure of avian orthoreovirus virion by electron cryomicroscopy and image reconstruction. *Virology.* 343:25-35; 2005.

28. Su YP, Su BS, Shien JH, Liu HJ, Lee LH. The sequence and phylogenetic analysis of avian reovirus genome segments M1, M2, and M3 encoding the minor core protein mu A, the major outer capsid protein mu B, and the nonstructural protein mu NS. *J Virol Methods.* 133:146-157; 2006.

29. Huang DD, Nugent MA, Rosenberger JK, Schnitzer TJ. Association of avian reovirus M and S genes with viral behavior in vivo. II. Viral pathogenicity. *Avian Diseases.* 31:446-454; Language of Summary: Spanish; Castilian. 1987.

30. Egana-Labrin S, Hauck R, Figueroa A, Stoute S, Shivaprasad HL, Crispo M, Corsiglia C, Zhou H, Kern C, Crossley B*, et al.* Genotypic Characterization of Emerging Avian Reovirus Genetic Variants in California. *Sci Rep-Uk.* 9: English. 2019.

31. Dina Zita M, Phillips MB, Stuart JD, Kumarapeli AR, Snyder AJ, Paredes A, Sridharan V, Boerma M, Danthi P, Boehme KWJJoV. The M2 Gene Is a Determinant of Reovirus-Induced Myocarditis. 96:e01879-21; 2022.

32. Ayalew LE, Ahmed KA, Mekuria ZH, Lockerbie B, Popowich S, Tikoo SK, Ojkic D, Gomis S. The dynamics of molecular evolution of emerging avian reoviruses through accumulation of point mutations and genetic re-assortment. *Virus Evol.* 6: English. 2020.

33. Martínez-Costas J, Grande A, Varela R, García-Martínez C, Benavente J. Protein architecture of avian reovirus S1133 and identification of the cell attachment protein. *J Virol.* 71:59-64; 1997.

34. Touris-Otero F, Martinez-Costas J, Vakharia VN, Benavente J. Avian reovirus nonstructural protein microNS forms viroplasm-like inclusions and recruits protein sigmaNS to these structures. *Virology.* 319:94-106; 2004.

35. Broering TJ, Arnold MM, Miller CL, Hurt JA, Joyce PL, Nibert MLJJov. Carboxyl-proximal regions of reovirus nonstructural protein μNS necessary and sufficient for forming factory-like inclusions. 79:6194-6206; 2005.

36. Brandariz-Nunez A, Menaya-Vargas R, Benavente J, Martinez-Costas J. Avian Reovirus mu NS Protein Forms Homo-Oligomeric Inclusions in a Microtubule-Independent Fashion, Which Involves Specific Regions of Its C-Terminal Domain. *J Virol.* 84:4289-4301; 2010.

37. Tourís-Otero F, Cortez-San Martín M, Martínez-Costas J, Benavente JJJomb. Avian reovirus morphogenesis occurs within viral factories and begins with the selective recruitment of sigmaNS and lambdaA to microNS inclusions. 341:361-374; 2004.

38. Parker JS, Broering TJ, Kim J, Higgins DE, Nibert MLJJov. Reovirus core protein μ2 determines the filamentous morphology of viral inclusion bodies by interacting with and stabilizing microtubules. 76:4483-4496; 2002.

39. Marin-Lopez A, Barreiro-Pineiro N, Utrilla-Trigo S, Barriales D, Benavente J, Nogales A, Martinez-Costas J, Ortego J, Calvo-Pinilla E. Cross-protective immune responses against African horse sickness virus after vaccination with protein NS1 delivered by avian reovirus muNS microspheres and modified vaccinia virus Ankara. *Vaccine.* 38:882-889; English. 2020.

40. Barreiro-Piñeiro N, Pose-Boirazian T, Menaya-Vargas R, Martínez-Costas JM. Production and Purification of Candidate Subunit Vaccines by IC-Tagging Protein Encapsulation. *Vaccine Technologies for Veterinary Viral Diseases*. Springer. p. 27-40; 2022.

41. Bodelón G, Labrada La, Martínez-Costas J, Benavente J. The avian reovirus genome segment S1 is a functionally tricistronic gene that expresses one structural and two nonstructural proteins in infected cells. *Virology.* 290:181-191; 2001.

42. Shmulevitz M, Duncan RJTEj. A new class of fusion-associated small transmembrane (FAST) proteins encoded by the non-enveloped fusogenic reoviruses. 19:902-912; 2000.

43. Bodelón G, Labrada La, Martínez-Costas J, Benavente J. Modification of Late Membrane Permeability in Avian Reovirus-infected Cells VIROPORIN ACTIVITY OF THE S1-ENCODED NONSTRUCTURAL p10 PROTEIN. *The Journal of biological chemistry.* 277:17789-17796; 2002.

44. Shmulevitz M, Corcoran J, Salsman J, Duncan R. Cell-cell fusion induced by the avian reovirus membrane fusion protein is regulated by protein degradation. *J Virol.* 78:5996-6004; 2004.

45. Chen X, He Z, Fu M, Wang Y, Wu H, Li X, Cao H, Zheng SJJJov. The E3 ubiquitin ligase Siah-1 suppresses avian reovirus infection by targeting p10 for degradation. 92:e02101-17; 2018.

46. Chi PI, Huang WR, Lai IH, Cheng CY, Liu HJ. The p17 Nonstructural Protein of Avian Reovirus Triggers Autophagy Enhancing Virus Replication via Activation of Phosphatase and Tensin Deleted on Chromosome 10 (PTEN) and AMP-activated Protein Kinase (AMPK), as well as dsRNA-dependent Protein Kinase (PKR)/eIF2 alpha Signaling Pathways. *J Biol Chem.* 288:3571-3584; 2013.

47. Chiu H-C, Huang WR, Wang Y-Y, Li JY, Liao T-L, Nielsen BL, Liu H-JJJoV. Heterogeneous nuclear ribonucleoprotein A1 and lamin A/C modulate nucleocytoplasmic shuttling of avian reovirus p17. 93:e00851-19; 2019.

48. Liu H-J, Lin P-Y, Lee J-W, Hsu H-Y, Shih W-L. Retardation of cell growth by avian reovirus p17 through the activation of p53 pathway. *Biochemical and biophysical research communications.* 336:709-715; 2005.

49. Jose Marti´Nez-Costas AG, Rube´N Varela, Concepcio´N Garci´A-Marti´Nez, And Javier Benavente*. Protein Architecture of Avian Reovirus S1133 and Identification of the Cell Attachment Protein. *J Virol.* 71: 1997.

50. Grande A, Rodríguez E, Costas C, Everitt E, Benavente J. Oligomerization and cell-binding properties of the avian reovirus cell-attachment protein sigmaC. *Virology.* 274:367-377; 2000.

51. Calvo PG, Fox GC, Parrado XLH, Llamas-Saiz AL, Costas C, Martínez-Costas J, Benavente J, van Raaij MJJJomb. Structure of the carboxy-terminal receptor-binding domain of avian reovirus fibre sigmaC. 354:137-149; 2005.

52. Shapouri MRS, Arella M, Silim A. Evidence for the multimeric nature and cell binding ability of avian reovirus sigma 3 protein. *The Journal of general virology.* 77:1203-1210; 1996.

53. Goldenberg D, Lublin A, Rosenbluth E, Heller ED, Pitcovski JJV. Optimized polypeptide for a subunit vaccine against avian reovirus. 34:3178-3183; 2016.

54. Shih WL, Hsu HW, Liao MH, Lee LH, Liu HJ. Avian reovirus sigma C protein induces apoptosis in cultured cells. *Virology.* 321:65-74; 2004.

55. Uma R, Kataria M, Rahul S, Kataria JM. Anti-neoplastic effect of avian reovirus a C protein on Rous sarcoma virus-induced tumors in chicken. *Acta Virol.* 57:69-74; English. 2013.

56. Lin PY, Liu HJ, Chang CD, Chang CI, Hsu JL, Liao MH, Lee JW, Shih WL. Avian reovirus S1133-induced DNA damage signaling and subsequent apoptosis in cultured cells and in chickens. *Arch Virol.* 156:1917-29; 2011.

57. Ping-Yuan L, Hung-Jen L, Meng-Jiun L, Feng-Ling Y, Hsue-Yin H, Jeng-Woei L, Wen-Ling S. Avian reovirus activates a novel proapoptotic signal by linking Src to p53. *Apoptosis.* 11:2179-93; 2006.

58. Zhang Z, Lin W, Li X, Cao H, Wang Y, Zheng SJ. Critical role of eukaryotic elongation factor 1 alpha 1 (EEF1A1) in avian reovirus sigma-C-induced apoptosis and inhibition of viral growth. *Arch Virol.* 160:1449-61; 2015.

59. Vázquez-Iglesias L, Lostale-Seijo I, Martínez-Costas J, Benavente JJV. Different intracellular distribution of avian reovirus core protein sigmaA in cells of avian and mammalian origin. 432:495-504; 2012.

60. Xu W, Patrick MK, Hazelton PR, Coombs KMJJov. Avian reovirus temperature-sensitive mutant tsA12 has a lesion in major core protein σA and is defective in assembly. 78:11142-11151; 2004.

61. Huang W-R, Li J-Y, Liao T-L, Yeh C-M, Wang C-Y, Wen H-W, Hu N-J, Wu Y-Y, Hsu C-Y, Chang Y-KJVm. Molecular chaperone TRiC governs avian reovirus replication by protecting outer-capsid protein σC and inner core protein σA and non-structural protein σNS from ubiquitin-proteasome degradation. 264:109277; 2022.

62. Martinez-Costas J, Gonzalez-Lopez C, Vakharia VN, Benavente J. Possible involvement of the double-stranded RNA-binding core protein sigma A in the resistance of avian reovirus to interferon. *J Virol.* 74:1124-1131; English. 2000.

63. Xie LJ, Xie ZX, Wang S, Deng XW, Xie ZQ. Study of the activation of the PI3K/Akt pathway by the motif of sigma A and sigma NS proteins of avian reovirus. *Innate Immun.* 26:312-318; English. 2020.

64. Yin HS, Shieh HK, Lee LH. Characterization of the double-stranded RNA genome segment S3 of avian reovirus. *Journal of Virological Methods.* 67:93-101; English. 1997.

65. Wickramasinghe R, Meanger J, Enriquez CE, Wilcox GEJV. Avian reovirus proteins associated with neutralization of virus infectivity. 194:688-696; 1993.

66. Lin YH, Lee LH, Shih WL, Hu YC, Liu HJ. Baculovirus surface display of sigmaC and sigmaB proteins of avian reovirus and immunogenicity of the displayed proteins in a mouse model. *Vaccine.* 26:6361-7; 2008.

67. Yang ZJ, Wang CY, Lee LH, Chuang KP, Lien YY, Yin HS, Tong DW, Xu XG, Liu HJ. Development of ELISA kits for antibodies against avian reovirus using the sigma C and sigma B proteins expressed in the methyltropic yeast Pichia pastoris. *J Virol Methods.* 163:169-174; 2010.

68. Majumder S, Chauhan TKS, Nandi S, Goswami PP, Tiwari AK, Dhama K, Mishra BP, Kumar D. Development of a recombinant sigma B protein based dot-ELISA for the diagnosis of avian reovirus (ARV). *J Virol Methods.* 257:69-72; English. 2018.

69. Yin CH, Qin LT, Sun MY, Gao YL, Qi XL, Gao HL, Wang YQ, Jang LL, Wang XM. Identification of a linear B-Cell epitope on avian reovirus protein sigmaC. *Virus research.* 178:530-534; English. 2013.

70. Praharaj MR, Sahoo AP, Chauhan TK, Gandham RK, Saxena S, Agarwal RK, Dhama K, Mishra B, Marriappan AK, Tiwari AKJO. In vitro study on role of σB protein in avian reovirus pathogenesis. 9:19569; 2018.

71. Touris-Otero F, Cortez-San Martin M, Martinez-Costas J, Benavente J. Avian reovirus morphogenesis occurs within viral factories and begins with the selective recruitment of sigmaNS and lambdaA to microNS inclusions. *J Mol Biol.* 341:361-74; 2004.

72. Touris-Otero F, Martinez-Costas J, Vakharia VN, Benavente J. Characterization of the nucleic acid-binding activity of the avian reovirus non-structural protein sigma NS. *J Gen Virol.* 86:1159-1169; 2005.

73. Borodavka A, Ault J, Stockley PG, Tuma R. Evidence that avian reovirus sigma NS is an RNA chaperone: implications for genome segment assortment. *Nucleic Acids Res.* 43:7044-7057; 2015.

74. Lee CH, Raghunathan K, Taylor GM, French AJ, Tenorio R, Fernández de Castro I, Risco C, Parker JS, Dermody TSJM. Reovirus Nonstructural Protein σNS Recruits Viral RNA to Replication Organelles. 12:e01408-21; 2021.

75. Fahey J, Crawley J. Studies on chronic respiratory disease of chickens II. Isolation of a virus. *Canadian journal of comparative medicine*

veterinary science. 18:13; 1954.

76. Olson N, Kerr KJAd. Some characteristics of an avian arthritis viral agent. 10:470-476; 1966.

77. Lu H, Tang Y, Dunn PA, Wallner-Pendleton EA, Lin L, Knoll EA. Isolation and molecular characterization of newly emerging avian reovirus variants and novel strains in Pennsylvania, USA, 2011–2014. *Journal of Scientific Reports.* 5:1-11; 2015.

78. Ayalew LE, Gupta A, Fricke J, Ahmed KA, Popowich S, Lockerbie B, Tikoo SK, Ojkic D, Gomis S. Phenotypic, genotypic and antigenic characterization of emerging avian reoviruses isolated from clinical cases of arthritis in broilers in Saskatchewan, Canada. *Sci Rep-Uk.* 7: English. 2017.

79. De la Torre D, Astolfi-Ferreira CS, Chacon RD, Puga B, Ferreira AJP. Emerging new avian reovirus variants from cases of enteric disorders and arthritis/tenosynovitis in Brazilian poultry flocks. *Br. Poult. Sci.* 62:361-372; English. 2021.

80. Goldenberg D, Pasmanik-Chor M, Pirak M, Kass N, Lublin A, Yeheskel A, Heller D, Pitcovski J. Genetic and antigenic characterization of sigma C protein from avian reovirus. *Avian Pathol.* 39:189-99; 2010.

81. Du X, Ding M, Wu Q, Li C, Guo H, Liu G, Chen Z. Characterization of a P18 protein in the S1 segment of the novel duck reovirus genome. *Acta Virol.* 64:59-66; English. 2020.

82. Chen XM, Li TT, Chen XD, Li CX, Lin WW, Liu HY, Song SP, Bai XF, Zhang Y. Characterization of Monoclonal Antibodies against sigma A Protein and Cross-Reactive Epitope Identification and Application for Detection of Duck and Chicken Reovirus Infections. *Pathogens.* 8: English. 2019.

83. Jiang XN, Lin Y, Yang J, Wang HZ, Li C, Teng XY, Tang Y, Diao YX. Genetic characterization and pathogenicity of a divergent broiler-origin orthoreovirus causing arthritis in China. *Transbound Emerg Dis.* 00:1-11; 2020.

84. Palomino-Tapia V, Mitevski D, Inglis T, van der Meer F, Abdul-Careem MF. Molecular characterization of emerging avian reovirus variants isolated from viral arthritis cases in Western Canada 2012-2017 based on partial sigma (sigma)C gene. *Virology.* 522:138-146; 2018.

85. Mirbagheri SA, Hosseini H, Ghalyanchilangeroudi A. Molecular characterization of avian reovirus causing tenosynovitis outbreaks in broiler flocks, Iran. *Avian Pathology.* 49:15-20; English. 2020.

86. Mirzazadeh A, Abbasnia M, Zahabi H, Hess M. Genotypic characterization of two novel avian orthoreoviruses isolated in Iran from broilers with viral arthritis and malabsorption syndrome. *Iran J Vet Res.* 23:74; 2022.

87. Troxler S, Rigomier P, Bilic I, Liebhart D, Prokofieva I, Robineau B, Hess M. Identification of a new reovirus causing substantial losses in broiler production in France, despite routine vaccination of breeders. *Veterinary Record.* 172:556-+; 2013.

88. Dawe W, Kapczynski D, Linnemann E, Gauthiersloan V, Sellers H. Analysis of the immune response and identification of antibody epitopes against the sigma C protein of avian orthoreovirus following immunization with live or inactivated vaccines. *Avian Diseases.* 66:465-478; 2022.

89. van der Heide L. The history of avian reovirus. *Avian diseases.* 44:638-641; 2000.

90. De la Torre D, Astolfi-Ferreira CS, Chacón R, Puga B, Piantino Ferreira A. Emerging new avian reovirus variants from cases of enteric disorders and arthritis/tenosynovitis in Brazilian poultry flocks. *Br. Poult. Sci.* 62:361-372; 2021.

91. Liu R, Luo D, Gao J, Li K, Liu C, Qi X, Cui H, Zhang Y, Wang S, Wang X*, et al.* A Novel Variant of Avian Reovirus Is Pathogenic to Vaccinated Chickens. *Viruses.* 15:1800; 2023.

92. Ayalew LE, Gupta A, Fricke J, Ahmed KA, Popowich S, Lockerbie B, Tikoo SK, Ojkic D, Gomis SJSr. Phenotypic, genotypic and antigenic characterization of emerging avian reoviruses isolated from clinical cases of arthritis in broilers in Saskatchewan, Canada. 7:1-13; 2017.

93. Palomino-Tapia V, Nickel L, Schlegel B, Mitevski D, Inglis T, Abdul-Careem MF. Review of viral arthritis in Canada. *Avian Diseases.* 66:452-458; 2022.

94. Perelman B, Krispin H, Solomon A, Elrom K, Farnoushi Y. Use of Controlled Exposure as a Novel Method for Reovirus Arthritis/Tenosynovitis Prevention. A Preliminary Report. *Isr. J. Vet. Med.* 74:163-172; English. 2019.

95. Goldenberg D. Avian reovirus in Israel, variants and vaccines—A review. *Avian Diseases.* 66:447-451; 2022.

96. Kumar R, Porter RE, Mor SK, Goyal SM. Efficacy and Immunogenicity of Recombinant Pichinde Virus-Vectored Turkey Arthritis Reovirus Subunit Vaccine. *Vaccines.* 10:486; 2022.

97. Wang N, Li J, Wang Y, Wang Y, Zhang D, Shi C, Li Y, Bergmann SM, Mo X, Yin J. Recombinant lactococcus lactis expressing grass carp reovirus VP6 induces mucosal immunity against grass carp reovirus infection. *Frontiers in Immunology.* 13:914010; 2022.

98. Dhanwani R, Zhou Y, Huang Q, Verma V, Dileepan M, Ly H, Liang Y. A novel live pichinde virus-based vaccine vector induces enhanced humoral and cellular immunity after a booster dose. *J Virol.* 90:2551-2560; 2016.

99. Song S, Li P, Zhang R, Chen J, Lan J, Lin S, Guo G, Xie Z, Jiang S. Oral vaccine of recombinant Lactococcus lactis expressing the VP1 protein of duck hepatitis A virus type 3 induces mucosal and systemic immune responses. *Vaccine.* 37:4364-4369; 2019.

100. Lin KH, Hsu AP, Shien JH, Chang TJ, Liao JW, Chen JR, Lin CF, Hsu WL. Avian reovirus sigma C enhances the mucosal and systemic immune responses elicited by antigen-conjugated lactic acid bacteria. *Vaccine.* 30:5019-29; 2012.

101. Wu H, Williams Y, Gunn K, Singh N, Locy R, Giambrone J. Yeast-derived sigma C protein-induced immunity against avian reovirus. *Avian diseases.* 49:281-284; 2005.

102. Chang C-C, Liu H-J. Plant-made vaccines against avian reovirus. *Prospects of Plant-Based Vaccines in Veterinary Medicine.*209-223; 2018.

103. Huang L-K, Liao S-C, Chang C-C, Liu H-J. Expression of avian reovirus σC protein in transgenic plants. *J Virol Methods.* 134:217-222; 2006.

104. Lu S-W, Wang K-C, Liu H-J, Chang C-D, Huang H-J, Chang C-C. Expression of avian reovirus minor capsid protein in plants. *J Virol Methods.* 173:287-293; 2011.

105. Wu HZ, Scissum-Gunn K, Singh NK, Giambrone JJ. Toward the Development of a Plant-Based Vaccine Against Reovirus. *Avian Diseases.* 53:376-381; English. 2009.

106. Yu K, Ti J, Lu X, Pan L, Liu L, Gao Y, Guo X, Hu F, Liu C, Ma X. Novel duck reovirus exhibits pathogenicity to specific pathogen-free chickens by the subcutaneous route. *Sci Rep-Uk.* 11:11769; 2021.

107. Yang H, Zhang W, Wang M, Yuan S, Zhang X, Wen F, Guo J, Mei K, Huang S, Li Z. Characterization and pathogenicity evaluation of recombinant novel duck reovirus isolated from Southeast China. *Front Vet Sci.* 10:1124999; 2023.

108. Wang S, Lin FQ, Cheng XX, Wang JX, Zhu XL, Xiao SF, Zheng M, Huang MQ, Chen SY, Chen SL. The genomic constellation of a novel duck reovirus strain associated with hemorrhagic necrotizing hepatitis and splenitis in Muscovy ducklings in Fujian, China. *Mol Cell Probe.* 53: English. 2020.

109. Bi Z, Zhu Y, Chen Z, Li C, Wang Y, Wang G, Liu G. Induction of a robust immunity response against novel duck reovirus in ducklings using a subunit vaccine of sigma C protein. *Sci Rep-Uk.* 6:39092; 2016.

110. Yan H, Xu G, Zhu Y, Xie Z, Zhang R, Jiang S. Isolation and characterization of a naturally attenuated novel duck reovirus strain as a live vaccine candidate. *Veterinary Microbiology.* 261:109214; 2021.

111. Kuntz-Simon G, Blanchard P, Cherbonnel M, Jestin A, Jestin V. Baculovirus-expressed muscovy duck reovirus σC protein induces serum neutralizing antibodies and protection against challenge. *Vaccine.* 20:3113-3122; 2002.

112. Le Gall-Recule G, Cherbonnel M, Arnauld C, Blanchard P, Jestin A, Jestin V. Molecular characterization and expression of the S3 gene of muscovy duck reovirus strain 89026. *J. Gen. Virol.* 80:195-203; 1999.

113. Yin Q, Luo W, Mallajosyula V, Bo Y, Guo J, Xie J, Sun M, Verma R, Li C, Constantz CM*, et al.* A TLR7-nanoparticle adjuvant promotes a broad immune response against heterologous strains of influenza and SARS-CoV-2. *Nat Mater.* 22:380-390; 2023.

CHAPTER 2

SEROLOGIC RELATEDNESS OF AVIAN REOVIRUS FIELD ISOLATES REPRESENTING ESTABLISHED GENETIC CLUSTERS[1]

[1] **Oluwayinka, Olatunde and [1]Holly S. Sellers.** To be submitted to *Avian Diseases.*

Keywords: Avian Reovirus, Serotypes, Virus Neutralization, Hyperimmune Serum

Abbreviations: ARV – Avian reovirus; CAV – Chicken anemia virus**;** CELiC – Chicken embryo liver cell**;** ELISA – Enzyme linked immunosorbent assay**;** GC – Genotypic cluster**;** GMT – Geometric mean titer**;** IBDV – Infectious bursal disease virus**;** IBV – Infection bronchitis virus**;** NDV – Newcastle disease virus**;** RT-PCR – Reverse transcriptase polymerase chain reaction; SPF – Specific pathogen free**;** VN – Virus neutralization

Summary

Avian reovirus (ARV) infections cause diseases of significant economic importance in commercial poultry flocks across the US and beyond. Since 2011, there has been a rise in ARV-induced tenosynovitis among the progeny of vaccinated breeders in the U.S., suggesting a decline in the efficacy of commercial vaccines. This challenge is further compounded by the virus's rapid evolution, as evidenced by the sustained isolation of genetic variants. To date, seven genotypic clusters (GCs) of variant ARVs have been identified. However, their serologic relatedness remains unclear, making it uncertain whether genetic clustering reflects antigenic relationship. This necessitates a comprehensive antigenic characterization of field isolates across the seven GCs to better understand their serological relationships.

In this study, selected field isolates representing the seven defined GCs and 2 subclusters within each of GCs 1 to 3 were plaque purified three times on primary chicken embryo liver cells. Clonal isolates were subsequently administered to 3-week-old SPF chickens in a series of live and inactivated injections to produce strain specific hyperimmune serum two-way cross virus neutralization (VN) assays were performed and Archetti and Horsfall (1) R values were calculated to determine antigenic relatedness.

Homologous VN titers ranged from 512 to 1024 for all isolates, except for 143572 (the GC 6 representative strain), which exhibited a lower titer of 256. Cross VN assays revealed heterologous VN titers ranging from 0 to 45, while R values (expressed as percentages) varied between 0.3% and 3.8%. Low cross VN titers and low R values indicate serotype differences among the viral isolates analyzed.

In conclusion, results generated in this study provide direct evidence that GCs 1-7 represent distinct serotypes and that subclusters within these GCs likely represent separate serotypes.

Furthermore, while this study assessed serological relatedness *in vitro*, our findings provide empirical evidence that the immunity induced by commercial ARV vaccines—represented by strain S1133 in this study—does not effectively neutralize circulating field variants irrespective of their GC.

Introduction

ARV is of significant economic importance in poultry production, both in the United States and globally (2-6). It is associated with various clinical syndromes, including viral arthritis/tenosynovitis, runting-stunting syndrome, enteritis, hepatitis, and malabsorption syndrome (7, 8). Among these, ARV is the definitive cause of viral arthritis/tenosynovitis, as established in previous studies (9-11). In affected flocks, viral arthritis presents as lameness, often accompanied by bilateral or unilateral swelling of the hock joint. Protection against this disease is primarily achieved through vaccination, typically employing a prime-boost strategy that combines live modified and inactivated vaccines. The primary goal of these vaccination regimens is to maximize antibody levels in breeding hens, ensuring the passive transfer of maternal immunity to progeny. This approach provides early protection to broilers during their most vulnerable period, reducing the risk of clinical disease manifestation (12).

Avian reoviruses (ARV) belong to the genus *Orthoreovirus*. They are non-enveloped, double-stranded RNA (dsRNA) virus with an icosahedral capsid. The dsRNA genome consist of 10 segments that are categorized based on their electrophoretic mobility into three groups: large (L1–L3), medium (M1–M3), and small (S1–S4) (13). Together, the genome encodes 12 post-translational products, with each segment encoding a single protein except for the S1 segment, which is tricistronic (14). The third open reading frame (ORF) of S1 encodes the σC protein, a minor outer capsid protein mediates host cell attachment and contains multiple neutralizing epitopes (15). Sequences of the σC protein serve as the basis for molecular typing of ARV isolates, with seven distinct genotypic clusters (GCs) described, to date (16, 17).

Historically, commercial vaccines derived from S1133 strain were widely used for ARV control (18). Developed in the late 1970s, these vaccines were initially effective at preventing ARV

infections. However, a retrospective analysis of field strains of ARV isolated from Europe, Asia, and Australia between 1980 and 2000 indicates that vaccine variants were already circulating in the 1980s. (16). In the United State, an upsurge in the isolation of ARV from cases of tenosynovitis in commercial flock from vaccinated breeders was reported in 2012(2). Together, these findings highlight the inadequacy of protection provided by commercial vaccines. Given the continued emergence of variant ARV strains, it is essential to define the serological relatedness of circulating isolates and evaluate the effectiveness of the immunity provided by S1133-based vaccines against isolates across the seven GCs of ARV.

Earlier studies that attempted to antigenically characterize ARV strains were conducted before the establishment of the widely accepted σC-based molecular typing scheme, making it difficult to contextualize their findings within the current genotypic clusters (19-22). Therefore, this study aims to determine the antigenic relatedness of variant field isolates representing the seven genotypic clusters (GCs) and selected subclusters within three GCs, notably subcluster 1.1, represented by S1133, which includes strains used in most commercial vaccine preparations

Materials and methods

Plaque purification of representative avian reovirus field isolates from each of the seven genotypic clusters. Reovirus field isolates from GCs 1-7 were selected for plaque purification (Table 2.1). These field isolates include 96139, a strain which belongs to GC 1, subcluster 1.3, (S1133 a strain frequently used in commercial vaccine preparation belongs to GC 1 subcluster 1.1). Additionally, representative isolates were selected from two subclusters within GCs 2 and 3, while a single strain was selected from each of GCs 4 through 7 (Fig. 2.1). Plaque purification of reovirus field isolates was performed as previously described (Sellers, 2016). Briefly, 10-fold dilutions of each field isolate, from 10^{-1} to 10^{-6}, were inoculated onto confluent

monolayers of primary chicken embryo liver cells (CELiC) in 35mm plates and allowed to adsorb at 37C + 5% CO2 for 1 hour. Virus inoculum was removed and 2 ml of a mixture consisting of 2 ml of a 1:1 mixture of M199/F10 (5% calf serum) and 3% SeaPlaque Agarose was added to each plate and incubated at 37^{o}C + 5% CO_2. At 48 hours post-inoculation, a 2% neutral red solution was added to each plate, incubated for 45 minutes at 37C + 5% CO2, then removed by aspiration. Plates were further incubated for 2 hours then evaluated by light microscopy. Plaques were picked from dilution plates containing well-spaced plaques using a sterile filter pipette tip, added to 0.5 ml F10/M199 media, vortexed and kept at 4^{o}C overnight then frozen at -80^{o}C until further use. Plaques were then inoculated onto monolayers of primary CELiC in duplicate. A two ml volume of a 1:1 mixture of M199/F10 (5% calf serum) and 3% SeaPlaque Agarose was added to one plate and the plaque purification process was repeated while the other plate served as the expansion plate. A total of three rounds of plaque purification was carried out for each field isolate. The final plaque purified stock was expanded and titrated in primary CELiC then used as stock virus for hyperimmune serum production. Identity confirmation by reovirus σC RT-PCR/sequencing was performed on all of the plaque-purified stocks as previously described (16).

Production of strain specific hyperimmune serum in SPF chickens using each plaque-purified virus. Twenty-five, 3-week-old SPF chickens (SPAFAS, Norwich, CT USA) were used for production of hyperimmune serum for each plaque purified reovirus isolate. All birds were housed in Horsfall-Bauer isolation units with forced air under positive pressure. Prior to bird placement, feed was dispensed into tightly covered plastic vat labelled with colored stickers specific for each isolate for use throughout the study to prevent cross contamination/exposure between reovirus isolates. Hyperimmune serum was produced for two isolates at a time and individual lab personnel assigned to each virus group to prevent cross contamination. Birds in

each group were inoculated intraocularly with live plaque purified virus at 3 weeks of age with 10^4 TCID50/bird depending on the virus isolate. Reoviruses were inactivated with beta-propiolactone, dialyzed, and a water in oil emulsion was prepared with Montanide ISA 70 VG adjuvant (Seppic, Fairfield, NJ, USA). Birds were injected intramuscularly (via the breast muscle) with 0.5 ml of respective homologous oil emulsion vaccine at six weeks of age. Birds were bled at 3 weeks post-live and inactivated virus inoculation and serum tested by Reovirus ELISA and virus neutralization (VN) with homologous viruses to monitor reovirus specific antibody response. At nine weeks of age, if homologous VN titer was 256 or greater, birds were bled and serum was harvested from each bird. If the VN titer was below 256, inactivated virus inoculation was repeated. Individual serum samples from birds in each group were tested by VN with homologous virus, and serum samples with VN titers greater than 256 were pooled for stock serum. Each stock serum was streaked onto blood agar incubated at 37ºC for 5 days and was submitted for serological testing against: IBDV, NDV, IBV, CAV and REO to test for exposure to common avian pathogens and reovirus antibody levels. All procedures were approved by the Institutional Animal Care Use Committee (IACUC) [A2023 01-036-41-A)]

Utilizing the panel of hyperimmune serum in cross neutralization assays to determine antigenic relatedness of field isolates between and within each of the 7 GCs. VN assay with constant virus (100 TCID50/well) and serially diluted serum was performed in 96-well plate using primary chicken embryo liver cells (CeLic) prepared from 12-day-old specific pathogen free (SPF) embryos (23). Prior to setting up cross neutralization tests, the VN titer for each antiserum stock was determined with homologous antigen. Samples were tested in duplicate. The VN titer was defined as the reciprocal of the highest dilution that resulted in at least 75% inhibition of characteristic ARV cytopathic effect (CPE). A 75% CPE reduction endpoint was selected based

on the results of a series of repeated VN assays conducted at our lab (data not shown). This provided more distinct and reproducible results, particularly when titration plates were evaluated by different individuals allowing for greater consistency in endpoint determination.

Further, serum stocks with homologous VN titers greater than 512 were diluted to a maximum titer of 512 for use in cross VN assays. Two-way cross neutralization assays were conducted in triplicate in primary CeLic in 96-well plates using 100 TCID50/well of antigen. Using the homologous and heterologous titers of any two viruses being tested, antigenic relatedness (R) values were calculated for the pair using the method of Archetti and Horsfall (1) and evaluated as previously published (22) where R values between 0-10% reflect serotype differences; 11-32%, major subtype differences; 33-70%, minor subtype differences and little or no differences for R values greater than 70%.

Results

Plaque purification of representative avian reovirus field isolates from each of the seven GCs. A widely used approach for characterizing reovirus isolates involves genotyping based on RT-PCR amplification of the σC -encoding region within the S1 gene segment, followed by sequencing. In this study, a total of nine representative field isolates were selected across all GCs for plaque purification.

Plaque purification of the representative isolates listed in Table 2.1 was successfully achieved, and their identities were confirmed via RT-PCR amplification of the sigma C-encoding region, followed by phylogenetic analysis of sequences (Fig. 2.1).

Isolates belonging to subclusters within the same GC exhibited considerable genetic variation, with the highest amino acid sequence identity (84%) observed between the GC 3 isolates

included in this study. More genetic diversity was detected between isolates from different genotypic clusters (GCs), with sequence identity ranging from 62% to 47% (Table 2.2).

Furthermore, when compared to the vaccine strain S1133, extensive genetic variation was observed across all genotypic clusters (Table 2.2). This highlights the significant genetic diversity among circulating field isolates within and between the seven GCs.

Production of clonal hyperimmune serum using each plaque-purified field isolates in SPF chickens. A clonal isolate of each virus was successfully utilized to generate hyperimmune serum in SPF chickens. Screening for extraneous avian pathogens via ELISA and bacterial culture yielded negative results, confirming the absence of cross-contamination from external sources (Table 2.3).

Reovirus GMTs, measured using a commercial ELISA kit (IDEXX), were positive for all hyperimmune sera derived from field isolates. ELISA GMT values ranged from 3,387 to 25,530 (Table 2.4), confirming successful immunization.

Additionally, these findings provide direct evidence that at least one commercial reovirus ELISA kit (IDEXX) can detect group-specific antibodies across all known ARV GCs. Although not assessed in this study, it is likely that other commercial ELISA kits exhibit similar detection capabilities.

In homologous virus neutralization (VN) assays measuring type-specific antibody titers, most field isolates exhibited titers ranging from 512 to 1024. However, 143572, the GC 6 representative strain, had a titer of 256. In addition, S1133 antiserum (SPAFAS, Norwich, CT USA) had homologous VN titer of 2048 (Table 2.4).

Determination of antigenic relatedness R values. Heterologous VN titers for each stock revealed poor neutralization between reoviruses in each GC and within 2 subclusters of GCs 1 - 3

(Table 2.5), thus providing direct evidence that distinct serotypes exist between and within genotypes.

While direct examination of VN titers was sufficient to conclude the serotypic differences between and within GCs, R values were calculated for cross VN. Analysis reveals major serotype differences among the isolates examined with less than 3.8% serological relatedness observed for any two isolates (Table 2.6). In addition, major serotype differences were identified between isolates belonging to subclusters within three GCs: GC 1(s1133 and 96139), GC 2 (106761 and 107177) and GC 3 (99846 and 107008) (Table 2.6). This is not surprising, given the amino acid similarity between subcluster isolates in each of GCs 1- 3 was 79%, 70% and 84%, respectively (Table 2.3).

Discussion and Conclusion

Protection conferred by commercial vaccines is inadequate against circulating field strains of ARV. This necessitates a detailed antigenic characterization of ARV isolates to assess their relatedness and potential for cross-protection. A previous study (19) used virus neutralization and serology to evaluate ARV antigenic diversity comparing isolates form US and Europe with previously characterized Japanese (20) and U.S. (21) serotypes. Eleven distinct ARV serotypes were identified, demonstrating considerable antigenic diversity among the isolates. In another study, commercial vaccine strains showed only minor or no subtype differences (22).

In this study, hyperimmune serum was generated against representative strains from each of the seven GCs of ARV. These sera were then used to perform cross-neutralization assays among the strains, following the beta neutralization protocol. Our findings indicate that the prime/boost immunization strategy yielded high type-specific neutralization titers, as previously reported (15). Also, results reveal that all strains evaluated in this study lacked serological relatedness. Therefore,

this study presents, for the first time, direct evidence supporting distinct serotypes among the seven ARV genetic clusters, as well as between two subclusters within the GC 1 through GC 3 isolates. Additionally, the results show that hyperimmune serum produced against S1133, a strain common in commercial vaccines, failed to neutralize any strain evaluated in this study regardless of their GC. The observed lack of serological relatedness among the reoviruses evaluated is unsurprising, given the low amino acid similarity between the isolates.

This study contributes to a broader understanding of the immune response to ARV. In this study, a commercial ELISA kit coated with inactivated whole virus - IDEXX Reo Ab Test (IDEXX Laboratories, Westbrook, ME), was used to quantify group-specific ARV antibody titers in hyperimmune sera generated against isolates from each GC and selected subclusters. Notably, when these ELISA results are interpreted alongside the cross-neutralization data, which showed no cross-reactivity between GCs, it becomes apparent that ARV induces a robust humoral immune response in chickens, much of which is non-neutralizing.

A previous study has mapped virus-neutralizing epitopes to the σC protein (15), and our findings further support the notion that σC is likely the sole—or at least the predominant—target of neutralizing antibodies on the ARV surface since serologic differences were in conformity to σC phylogeny defined clustering for strains analyzed in this study. Together, these results suggest that while ARV elicits strong antibody responses detectable by whole-virus ELISA, effective virus neutralization is largely dependent on antibodies directed specifically against σC.

Further, this study focused on several representative isolates from each genotype, but did not encompass the full range of sub-lineage variants within each genotype. Given the impracticality of plaque purification and hyperimmune serum production for every field variant, emphasis should be placed on monitoring the emergence of prevalent GCs. With the emergence

of promising expression systems for the σC protein (24-27), this protein could serve as a basis for the development of ELISA assays tailored to prevalent lineages, potentially replacing the need for plaque purification of field isolates.

Moreover, the clonal antigen stocks and matched hyperimmune serum generated in this study will remain an essential tool in evaluation of neutralizing serum. Specifically, they are valuable for monitoring the effectiveness of autogenous reovirus vaccine programs in breeders and assessing maternal antibody transfer to progeny from vaccinated breeders. However, it is worth noting that in the absence of homologous live-attenuated reoviruses for priming, the duration of immunity of autogenous vaccines is expected to be shorter than that achieved with commercial live prime/boost with s1133. As a result, additional booster vaccinations with autogenous vaccines may be required to extend immunity and optimize vaccine efficacy.

Acknowledgement

This research was supported by the USA Poultry and Egg Association (Project No.: F693). I sincerely appreciate Erich Linneman, Vanessa Gauthiersloan, Nicholas Davis-fields, Amanda Greenway and Brandan Dixon for their excellent technical assistance and significant contribution towards making this study possible, and Dr Amal Mouhamed for her expert review of this manuscript.

Reference

1. Archetti I, Horsfall Jr FL. Persistent antigenic variation of Influenza A viruses after incomplete neutralization *in ovo* with heterologous immune serum. *The Journal of experimental medicine.* 92:441-462; 1950.

2. Sellers HS. Current limitations in control of viral arthritis and tenosynovitis caused by avian reoviruses in commercial poultry. *Vet Microbiol.* 206:152-156; 2017.

3. French D. Incidence and economic impact of reovirus in the poultry industries in the United States. *Avian Diseases.* 66:432-434; 2022.

4. Goldenberg D. Avian reovirus in Israel, variants and vaccines—A review. *Avian Diseases.* 66:447-451; 2022.

5. Palomino-Tapia V, Nickel L, Schlegel B, Mitevski D, Inglis T, Abdul-Careem MF. Review of viral arthritis in Canada. *Avian Diseases.* 66:452-458; 2022.

6. Troxler S, Rigomier P, Bilic I, Liebhart D, Prokofieva I, Robineau B, Hess M. Identification of a new reovirus causing substantial losses in broiler production in France, despite routine vaccination of breeders. *Veterinary Record.* 172:556-+; 2013.

7. Jones RC. Avian reovirus infections. *Rev Sci Tech (International Office of Epizootics).* 19:614-625; 2000.

8. Egana-Labrin S, Jerry C, Roh HJ, da Silva AP, Corsiglia C, Crossley B, Rejmanek D, Gallardo RA. Avian reoviruses of the same genotype induce different pathology in chickens. *Avian Diseases.* 65:530-540; 2021.

9. Walker ER, Friedman M, Olson N. Electron microscopic study of an avian reovirus that causes arthritis. *Journal of ultrastructure research.* 41:67-79; 1972.

10. Ngunjiri JM, Ghorbani A, Jang H, Waliullah S, Elaish M, Abundo MC, Mahesh KC, Taylor KJ, Porter RE, Lee CW. Specific-pathogen-free turkey model for reoviral arthritis. *Vet Microbiol.* 235:170-179; 2019.

11. Ayalew LE, Ahmed KA, Popowich S, Lockerbie BC, Gupta A, Tikoo SK, Ojkic D, Gomis S. Virulence of emerging arthrotropic avian reoviruses correlates with their ability to activate and traffic interferon-gamma producing cytotoxic CD8(+) T cells into gastrocnemius tendon. *Front Microbiol.* 13:869164; 2022.

12. Gamble T, Sellers H. Field control of avian reoviruses in commercial broiler production. *Avian Diseases.* 66:427-431; 2022.

13. Benavente J, Martínez-Costas J. Avian reovirus: structure and biology. *Virus research.* 123:105-119; 2007.

14. Benavente J, Martínez-Costas J. Early steps in avian reovirus morphogenesis. *Current topics in microbiology and immunology.* 309:67-85; 2006.

15. Dawe W, Kapczynski D, Linnemann E, Gauthiersloan V, Sellers H. Analysis of the immune response and identification of antibody epitopes against the sigma C protein of avian orthoreovirus following immunization with live or inactivated vaccines. *Avian Diseases.* 66:465-478; 2022.

16. Kant A, Balk F, Born L, Van Roozelaar D, Heijmans J, Gielkens A, Ter Huurne A. Classification of Dutch and German avian reoviruses by sequencing the sigma-C protein. *Veterinary research.* 34:203-212; 2003.

17. Sellers HS. Avian reoviruses from clinical cases of tenosynovitis: An overview of diagnostic approaches and 10-year review of isolations and genetic characterization. *Avian Diseases.* 66:420-426; 2022.

18. van der Heide L. The history of avian reovirus. *Avian diseases.* 44:638-641; 2000.

19. Wood G, Nicholas R, Hebert Ca, Thornton D. Serological comparisons of avian reoviruses. *Journal of comparative pathology.* 90:29-38; 1980.

20. Kawamura H, Shimizu F, Maeda Ma, Tsubahara H. Avian reovirus: its properties and serological classification. *National Institute of Animal Health Quarterly.* 5:115-124; 1965.

21. Sahu S, Olson N. Comparison of the characteristics of avian reoviruses isolated from the digestive and respiratory tract, with viruses isolated from the synovia. *American journal of veterinary research.* 36:847-850; 1975.

22. Giambrone J, Solano W. Serologic comparison of avian reovirus isolates using virus neutralization and an enzyme-linked immunosorbent assay. *Avian diseases.*678-680; 1988.

23. Hieronymus DR, Villegas P, Kleven S. Identification and serological differentiation of several reovirus strains isolated from chickens with suspected malabsorption syndrome. *Avian Diseases.*246-254; 1983.

24. Wu H, Smith L, Scissum-Gunn K, Giambrone J, Robertson B, Villafane R. Construction of epitope-based vaccine for avian reovirus. *Madridge J Clin Res.* 2:50-54; 2018.

25. Goldenberg D, Lublin A, Rosenbluth E, Heller ED, Pitcovski J. Optimized polypeptide for a subunit vaccine against avian reovirus. *Vaccine.* 34:3178-3183; 2016.

26. Minhas SK, Kamble NM, Kataria J, Mohan CM, Dey S. High-Yield xxpression and purification of recombinant σB protein of avian reovirus (ARV) in prokaryotic system. *Int. J. Curr. Microbiol. App. Sci.* 6:434-441; 2017.

27. Wang Y, Xu S, Chen X, Dou Y, Yang X, Hu Z, Wu S, Wang X, Hu J, Liu X. Single dose of recombinant baculovirus vaccine expressing sigma B and sigma C genes provides good protection against novel duck reovirus challenge in ducks. *Poultry Sci.* 104:104565; 2025.

Table 2. 1: Genotypic cluster identification of reovirus field isolates plaque-purified for hyperimmune serum production.

Genotypic Cluster	Representative Field Isolates
1.2	96139
2.1	106761
2.2	107177
3.1	99846
3.2	107008
4	108089
5	94826
6	143572
7	127720

Table 2. 2: Sigma C amino acid sequence identity values (%) between plaque purified reovirus field isolates and S1133

	S1133 GC 1.1	96139 GC 1.3	106761 GC 2.3	107177 GC 2.1	99846 GC 3.2	107008 GC 3.1	108089 GC 4	94826 GC 5	143572 GC 6	127720 GC 7
S1133	100	79	53	54	49	49	48	47	47	48
96139		100	54	57	52	51	51	51	49	49
106761			100	70	50	50	50	52	51	50
107177				100	53	53	50	53	50	50
99846					100	84	53	60	54	62
107008						100	52	50	55	62
108089							100	62	60	53
94826								100	60	50
143572									100	54
127720										100

Table 2. 3: Serological and bacteriological evaluation of pooled serum samples from each hyperimmune serum stock by ELISA (IDEXX) and blood agar culturing (Remel): Newcastle disease virus (NDV), Infectious bronchitis virus (IBV), Infectious bursal disease virus (IBDV), and Chicken anemia virus (CAV).

	ELISA				Bacteriology
Antisera stock	NDV	IBV	IBDV	CAV	Blood Agar
94826	NEG	NEG	NEG	NEG	No Growth
96139	NEG	NEG	NEG	NEG	No Growth
108089	NEG	NEG	NEG	NEG	No Growth
106761	NEG	NEG	NEG	NEG	No Growth
107008	NEG	NEG	NEG	NEG	No Growth
107177	NEG	NEG	NEG	NEG	No Growth
99846	NEG	NEG	NEG	NEG	No Growth
143572	NEG	NEG	NEG	NEG	No Growth
127720	NEG	NEG	NEG	NEG	No Growth

Table 2. 4: Geometric mean ELISA (IDEXX) antibody titers and homologous VN titers for the seven reovirus antisera stocks

Virus	Genetic Cluster	GMT Reovirus ELISA (IDEXX)	GMT of Homologous VN Reactions
S1133	GC 1.1	N/A	2048
96139	GC 1.3	17,519	512
107177	GC 2.1	14,711	512
106761	GC 2.3	17,286	1,024
107008	GC 3.1	11,005	512
99846	GC 3.2	9,339	1,024
108089	GC 4	11,028	512
94826	GC 5	25,530	512
143572	GC 6	3,387	256
127720	GC 7	10,444	512

Table 2. 5: Homologous and heterologous VN titers of plaque purified reovirus field isolates from each of the seven defined GC of ARV.

	Virus[A]									
Serum[B]	1133 GC 1.1	96139 GC 1.3	106761 GC 2.3	107177 GC 2.1	99846 GC3.2	107008 GC 3.1	108089 GC 4	94826 GC 5	143572 GC 6	127720 GC 7
1133	512	32	8	4	0	4	4	8	8	45
96139	2	512	2	4	0	2	8	8	0	4
106761	8	0	512	2	4	8	2	8	4	6
107177	0	0	32	512	0	4	0	32	0	2
99846	8	16	2	2	512	2	4	4	4	3
107008	4	4	2	4	2	512	0	0	0	11
108089	4	8	2	4	8	4	512	8	0	4
94826	2	0	4	8	2	8	8	512	0	4
143572	0	0	4	3	45	64	2	0	256	4
127720	0	0	11	6	4	0	0	0	0	512

[A]Virus at 10^2TCID/50µl

[B] Serum stock diluted to 512 if stock titer is greater

Table 2. 6: Serological relatedness (%), based on Archetti and Horsfall R-values, between reovirus field isolates and S1133.

	Virus									
Serum	1133 GC 1.1	96139 GC 1.3	106761 GC 2.3	107177 GC 2.1	99846 GC3.2	107008 GC 3.1	108089 GC 4	94826 GC 5	143572 GC 6	127720 GC 7
1133	100	1.6	1.6	0.4	0.6	0.8	0.8	0.8	0.8	1.3
96139		100	0.3	0.4	0.8	0.6	1.6	0.6	0.3	0.4
106761			100	1.6	0.6	0.8	0.4	1.1	1.1	1.6
107177				100	0.3	0.8	0.3	3.1	0.5	0.7
99846					100	0.3	1.1	0.6	3.8	0.7
10700						100	0.4	0.6	2.2	0.7
108089							100	1.6	0.4	0.4
94826								100	0.3	0.4
143572									100	0.6
127720										100

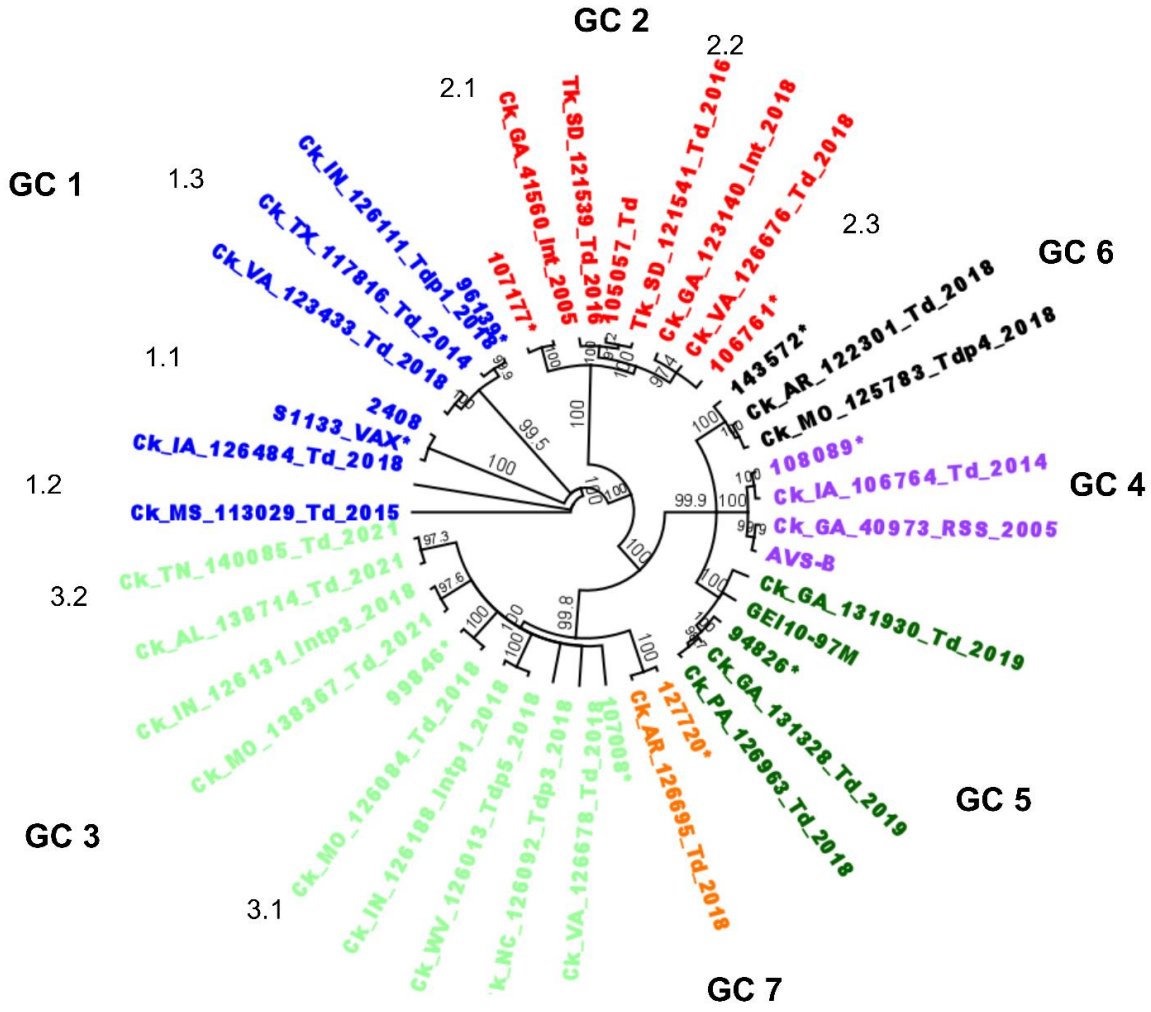

Fig. 2. 1: Phylogenetic analysis of partial σC sequences (310 amino acids) from nine plaque-purified field isolates, the S1133 vaccine strain, and 31 reference strains. On Geneious Prime 2024.0.5, multiple alignments were perfomed using Clusta Omega, and phylogenetic tree construction was conducted using the neighbor-joining method with 1000 bootstrap replicates. Viruses analyzed in this study are marked with an asterisk (*) following their names in the tree.

CHAPTER 3

IMPROVED RESOLUTION OF MIXED AVIAN REOVIRUS POPULATIONS IN CLINICAL SAMPLES USING A MINION-BASED SEQUENCING OF VIRAL σC AMPLICONS[1]

[1] **Oluwayinka, Olatunde and [1]Holly S. Sellers.** To be submitted to *Avian Diseases.*

Keywords: MinION, avian reovirus, amplicon sequencing, mixed viral populations

Abbreviations: ARV – Avian reovirus; DNA – Deoxyribonucleic acid; GC – Genotypic cluster; GPU – Graphics processing unit; GUI – Graphical user interface; MBAseq – MinION-based amplicon sequencing; MEGA – Molecular evolutionary genetics analysis; ML – Maximum likelihood; ONT – Oxford Nanopore Technology; PDRC – Poultry Diagnostic and Research Center; RNA – Ribonucleic acid; RT-PCR – Reverse transcriptase polymerase chain reaction

Summary

Genetic characterization of avian reovirus (ARV) field isolates traditionally relies on RT-PCR amplification of the viral Sigma C (σC)-encoding region within the S1 segment, followed by Sanger sequencing. However, estimates suggest that approximately 18% of field isolates contain mixed reovirus populations. Currently, resolving these mixed populations involves cloning the σC amplicons into a PCR cloning vector, transforming *E. coli* and selection of 5 individual clones for sequencing. While useful, this process may not detect all isolates in the mixed population given that a limited number of clones are sequenced.

In this study, a MinION-based amplicon sequencing method (MBAseq) was utilized for genetic characterization of mixed ARV populations from field isolates. Field isolates from 24 clinical case submissions to the Poultry Diagnostic and Research Center (PDRC) were evaluated. All submissions were previously characterized by RT-PCR followed by Sanger sequencing through routine diagnostic testing at the PDRC Virology laboratory. Twenty of the 24 samples contained mixed populations and were subsequently cloned and sequenced. The other 4 samples did not show evidence of the presence of mixed ARV populations. In this study, σC amplicons from all 24 isolates were processed into a sequencing library for analysis using the Oxford Nanopore Technologies (ONT) MinION sequencer. MBAseq revealed one additional reovirus sequence contig in one of four isolates not initially suspected of harboring mixed populations. In the 20 isolates initially characterized as containing mixed population by initial diagnostic sequencing, MBAseq confirmed all 43 contigs detected by PCR cloning and identified 13 additional contigs across 10 isolates, most of which had relatively low coverage. Pairwise analysis of counterpart contigs from both methods showed high concordance, with amino acid sequence similarity ranging from 94% to 100%.

In conclusion, our findings demonstrate that MBAseq can accurately resolve mixed ARV populations in field isolates, offering greater depth of resolution compared to conventional methods.

Introduction

The genus *Orthoreovirus*, within the family *Reoviridae,* includes avian reovirus (ARV) . ARV is widespread in poultry environments, making it challenging to discern whether its detection in diseased birds reflects an incidental finding or true causal role in disease. Nonetheless, ARV has also been linked to several disease conditions of poultry including malabsorption syndromes, hepatitis, myocarditis, enteritis and viral arthritis/ tenosynovitis. (1-6) However, among these, viral arthritis/tenosynovitis is the only condition for which ARV has been identified as the necessary etiologic agent (7-10). Clinical manifestations include lameness, swollen hocks and tendons, and in heavier birds, possible rupture of the gastrocnemius and digital flexor tendons (11, 12). Clinical outcomes lead to significant economic losses for poultry producers, due to decreased flock uniformity and increased condemnations at processing (13, 14) . Control strategies predominantly rely on vaccinating breeder flocks to enable passive transfer of antibodies to progeny, although early vaccination of broilers is included in some regimens (15). Most commercial vaccines are based on S1133 or closely related strains. However, increasing global reports of ARV isolation from tenosynovitis cases in progeny of vaccinated breeders highlight the inadequate protection conferred by these vaccines. (16-22). Genetic reassortment and point mutations serve as the primary mechanisms driving the emergence of variants (3, 23). In the U.S., marked increase in the isolation of variant strains was first observed in 2012 (12).

Molecular characterization of ARV relies on RT-PCR amplification and sequencing of the σC-encoding region of the genome. This σC-based typing scheme has classified ARV into seven genetic clusters (GCs). Additionally, three subclusters have been identified within GCs 1, 2, 4, and 5, while GCs 3 and 6 each contain two subclusters, reflecting the extensive genetic diversity of ARV (24).

One of the significant challenges in ARV isolation and characterization is the frequent presence of mixed viral populations in diagnostic samples. Data from the Poultry Diagnostic and Research Center (PDRC) indicate that 12–18% of positive samples analyzed between 2017 and 2021 contained mixed populations (12). Resolving these mixed populations is crucial for accurately tracking strains involved in outbreaks and effectively assessing vaccine efficacy, particularly in poultry operations utilizing autogenous vaccines. As part of the workflow for analysis of field isolates at the PDRC, the process of resolving heterogeneous ARV populations involve cloning σC amplicons, followed by Sanger sequencing of five clones. While useful, this process may not identify all isolates in the mixed population given that only five clones are sequenced.

Nanopore sequencing (Oxford Nanopore Technology [ONT]), a third-generation sequencing technology, has application in diagnosis of infectious diseases (25-32). Compared to Sanger and next generation sequencing (NGS), this technology provides notable benefits, including the generation of long reads, high throughput, real-time monitoring and analysis of sequencing run and the capability to directly sequence RNA or DNA molecules (33). ONT's MinION sequencer (34), offering the added advantage of portability and low startup investment has been successfully used for sequencing of pathogens in the field (35). MinION sequencing of targeted amplicons has been employed to characterize and detect several avian viral pathogens, including avian influenza (36, 37), infectious laryngotracheitis (38), Newcastle disease (39, 40), and infectious bronchitis viruses (28). Accordingly, this study aimed to evaluate a MinION-based amplicon sequencing (MbAseq) protocol for resolving mixed ARV populations in field isolates.

Materials and methods

Samples, σC RT-PCR, and mixed population screening. The twenty-four field isolates analyzed in this study were isolated from clinical case submissions to the PDRC (Table 3.1). Total RNA was extracted from each clarified virus supernatant using the 5X MagMax Pathogen RNA/DNA Kit (Thermo Fisher Scientific, Waltham, MA, USA) according to manufacturer's instructions. RNA was quantified using Nanodrop (Thermo Fisher Scientific, Waltham, MA, USA), aliquoted and stored at -80 until further use. RT-PCR was performed to amplify the σC-encoding region of the viral S1 segment, following previously described methods (16). The resulting PCR products were purified using the QiaQuick PCR Purification Kit (Qiagen, Hilden, Germany) and subsequently sequenced via Sanger sequencing. Sanger chromatograms were analyzed and presence of multiple nucleotides at any given position throughout the σC RT-PCR product were indicative of a mixed population.

PCR cloning and Sanger sequencing for resolving mixed ARV populations. Purified σC amplicons from samples identified to contain mixed populations were cloned and Sanger sequenced to resolve the ARV populations. Briefly, purified PCR products were cloned into the pCR2.1 TOPO vector (TOPO TA Cloning Kit, Invitrogen, Carlsbad, CA, USA) and transformed into One Shot TOP10 chemically competent *E. coli* (Invitrogen, Carlsbad, CA, USA). The transformed cells were then transferred to pre-warmed SOC medium and incubated with shaking at 37°C for one hour, followed by plating on LB agar supplemented with ampicillin. Five recombinant colonies were selected per sample. However, for sample 145549, an additional 15 colonies were analyzed to evaluate whether increased sampling could provide deeper resolution. Selected colonies were subsequently inoculated into fresh LB broth and incubated with shaking at 37°C overnight. Plasmid DNA was then extracted and sequenced by Sanger sequencing using gene

specific primers. Sequence chromatograms were viewed, trimmed, and assembled using SeqMan Ultra software (DNAstar v17.1, Lasergene, Madison, WI, USA).

MinION-based amplicon sequencing (MBAseq) protocol for resolution of mixed ARV populations. RT-PCR products of viral σC amplification from all samples were purified using AMPure beads (Beckman Coulter, Indianapolis, IN, USA) at a 1.4X ratio and quantified with a Qubit fluorometer using the Qubit dsDNA Broad Range kit (Thermo Fisher Scientific, Waltham, MA, USA). Amplicon library construction for all samples followed the ONT protocol for native barcoding (NBA-9170-v114-revN-15sep2022). Briefly, DNA concentrations were normalized to 200 fmol, and samples were end-repaired and dA-tailed using the NEBNext Ultra II End Repair/dA-tailing Module (New England Biolabs, Ipswich, MA, USA).

For barcoding, end repaired and dA-tailed σC amplicons from each field isolate were ligated to a unique native barcode from the SQK-NBD114.96 ligation sequencing kit (ONT, Oxford, UK) using the NEB Blunt/TA Ligase Master Mix (New England Biolabs, Ipswich, MA, USA). The barcoded samples were then pooled and purified using 0.4X of ONT-supplied AMPure XP beads. Adapter ligation was subsequently performed with the NEBNext Quick Ligation Module (New England Biolabs, Ipswich, MA, USA). The final library was quantified and loaded onto an R10.4.1 flow cell (FLO-MIN114) for sequencing on the MinION MK1b, following the manufacturer's instructions and using MinKNOW software version 24.06.16 for sequencing settings and monitoring. Post-run basecalling, demultiplexing, and adapter trimming were performed on a GPU-enabled computer using MinKNOW software.

Construction of custom σC library. A maximum likelihood (ML) phylogenetic tree was generated from 212 nucleotide sequences corresponding to the segment of the viral S1 gene that encodes the σC protein. The sequences, which include those from Sellers 2022 (24) and Kant *et*

al., 2003 (16) encompass the known GCs and subclusters of ARV. The ML tree was constructed using MEGA 11 with 1000 bootstrap replicates to ensure robust branch support. Based on the topology of this tree, the custom σC library was assembled by selecting one or two representative sequences for each ARV GC and subclusters.

Bioinformatics pipeline for nanopore amplicon sequencing analysis. The entire bioinformatics workflow for analyzing MbAseq reads, as depicted in Fig. 3.1, was executed using Geneious Prime 2024.0.5. The initial step involved importing a Fastq folder containing base called, demultiplexed, and adapter-trimmed reads with a minimum quality score of 8. Reads were filtered to remove short fragments, retaining only those between 900 bp and 1220 bp. The filtered reads were then mapped to a custom σC library using the Geneious mapper (fast/non-iterative mapping), and consensus sequences were derived from read clusters with an average coverage of at least 20X.

Consensus sequences from generated from filtered reads for each field isolate were aligned to identify identical or highly similar sequences using Muscle v5.1 (41). Consensus sequences within a GC that exhibited greater than 97% similarity and where differences were not due to the insertion of short sequence of nucleotide, were considered similar. In cases where similarity was 97% or below, or where short nucleotide insertions accounted for much of the dissimilarity, the mapping of the filtered reads to the custom library was repeated using the Geneious mapper with 5X iterative mapping option. Although computationally intensive, this iterative approach effectively resolved spurious insertions. The read clusters from this second-round mapping were then used for final consensus sequence generation.

Analysis of σC sequences generated by both methods. To assess the mean coverage of all σC contigs identified by MBAseq, unfiltered reads from each isolate were mapped to the corresponding σC sequences, and the mean coverage as computed by the Geneious Prime viewer,

was recorded for each contig. All unique σC sequences obtained by either MBAseq, PCR cloning with Sanger sequencing and direct Sanger sequencing of σC amplicons were further analyzed using Geneious Prime 2024.0.5. For the 20 field isolates that were determined to contain mixed populations , the predicted amino acid sequences of the σC contigs derived from both MBAseq and Sanger sequencing of PCR clones were aligned with Muscle 5.1 (41) to identify counterpart sequences—defined as those with greater than 90% amino acid identity. Subsequently, each pair of counterpart sequences was pairwise aligned to determine their precise amino acid sequence similarity.

Lastly, σC sequences generated in this study including those from MBAseq, Sanger sequencing of σC amplicons of four isolates without evidence of the presence of heterogenous ARV populations at initial diagnostic screening and Sanger of PCR clones generated from samples with mixed ARV populations, were phylogenetically analyzed. Clustal Omega was used for multiple sequence alignment and a phylogenetic tree was constructed using neighbor-joining method with a Jukes-Cantor model and 1000 bootstrap replicates.

Results

RT-PCR and screening for mixed populations. All 24 field isolates analyzed in this study were positive for ARV as determined by successful amplification and sequencing of the viral sigma C protein encoding region of the genome. However, following examination of Sanger sequence data from diagnostic σC sequencing, 20 field isolates were identified to contain heterogenous populations while 4 appeared to have single populations based on initial Sanger sequencing data (Table 3.1).

Performance of MBAseq on samples with unambiguous Sanger chromatograms. In this study, diagnostic Sanger sequencing of the σC gene from four ARV field isolates indicated

the presence of a single ARV population per isolate. These isolates were subsequently included in the MinION sequencing run to assess the platform's ability to detect low-abundance strains that may be missed by conventional Sanger sequencing of RT-PCR amplicons. MBAseq detected a single σC contig for each of three field isolates from this batch of four isolates, consistent with initial Sanger results. However, for one isolate (149064), MBAseq detected two σC contigs – one more than Sanger sequencing detected (Fig. 3.2). Coverage analysis showed that this additional contig (M_149064_2) had a relatively low coverage of 95X compared to the other contig with a counterpart from Sanger sequencing (M_149064_1) with over 18,000X mean coverage (Fig. 3.4), thus demonstrating that MBAseq is capable of identifying low-abundance ARV populations more effectively than Sanger sequencing of σC amplicons in isolates showing no evidence of presence mixed ARV populations from Sanger chormatograms.

Comparison of MBAseq and PCR cloning followed Sanger sequencing for resolving mixed ARV populations. Twenty field isolates previously identified as containing mixed ARV populations during initial screening were analyzed using PCR cloning and Sanger sequencing. Result shows that in 10 out of the 20 field isolates, the number of σC contigs identified by PCR cloning matched those detected by MBAseq. However, MBAseq identified a total of 13 additional unique σC contigs across the remaining 10 field isolates that were not detected by PCR cloning with Sanger Sequencing. Notably, in one of these field isolates (148807), MBAseq detected three additional σC contigs that were not identified through PCR cloning-Sanger sequencing (Fig. 3.3).

Analysis of σC sequences identified by both methods. As shown in Fig.3.4, when mean coverages of MBAseq-derived σC contigs are plotted in ascending order, all contigs lacking corresponding sequences from PCR cloning with Sanger sequencing appeared in the lower third of the chart indicating their relatively lower coverages compared to other σC sequences.

Nonetheless, several low coverage contigs were still identified by PCR cloning with Sanger sequencing, including the MBAseq contig with the lowest coverage - M_145549_2 (75X) (Fig. 3.4).

Additionally, pairwise alignment of amino acid sequences revealed that all σC sequences identified by PCR cloning in the 20 field isolates earlier determined to contain mixed ARV populations, had closely matching counterparts identified by MBAseq. The similarities between matched sequences ranged from 94% to 100%. Among the 43 matched pairs, 38 exhibited high pairwise similarity, ranging from 99% to 100% (Table 3.2). Further, phylogenetic analysis of σC sequences generated in this study clearly show that all counterpart contigs consistently cluster within the same GC regardless of their pairwise amino acid similarity between (Fig. 3.5). This indicates that MBAseq provides sufficient accuracy for precise characterization of constituent ARVs within a mixed population

Discussion and Conclusion

Coinfection of poultry flocks with multiple strains of ARV is common (12, 42). Factors that likely facilitate these coinfections include possible vertical transmission of multiple reoviruses from breeder flocks, the setting and hatching of eggs from multiple infected breeder flocks, and horizontal exposure among vertically infected chicks. Distinguishing individual strains within a heterogeneous ARV infection is crucial for effective epidemiological tracking of strains across outbreaks and for guiding the selection and monitoring of control interventions. Although protocols based on cloning of RT-PCR products followed by Sanger sequencing remain useful for resolving these heterogeneous viral populations in field isolates, they are likely limited in the depth

of resolution achievable since only a minute number of recombinant clones can feasibly be sequenced during diagnostic testing.

This study demonstrates the utility of a third-generation sequencing platform—ONT's MinION Sequencing—in resolving heterogeneous ARV populations within field isolates. We analyzed 24 ARV field isolates from clinical case submissions to the PDRC. Among these, Sanger sequencing data from four isolates lacked multiple or overlapping peaks indicative of presence of mixed ARV populations in the isolate. However, this does not necessarily imply the absence of mixed infections, as dominant high-abundance strains may mask low-abundance strains during Sanger sequencing of σC amplicons. Results generated in this study revealed that MBAseq detected two σC contigs in isolate 149064. One of the MBAseq-derived contigs matched the sequence reported by diagnostic Sanger sequencing of σC amplicons, while the other was unique. Notably, the unique contig (M_149064_2) exhibited a mean coverage depth of 95X, compared to over 18,000X for the contig (M_149064_1) with the matching counterpart. These findings indicate that MBAseq is capable of detecting strains present at low abundance or that are undetectable by direct Sanger sequencing of σC amplicons. MinION coverages have been shown to correlate strongly with virus abundance (as defined by RT-qPCR cycle threshold values) in clinical samples for other avian viral and bacterial pathogens (31).

Moreover, in the head-to-head comparison between MBAseq and PCR cloning for isolates containing multiple ARV strains from initial diagnostic sequencing, MBAseq not only produced results comparable to PCR cloning and Sanger sequencing but also detected additional contigs in 10 out of 20 samples. Most of these additional sequences exhibited relatively low coverages, further demonstrating the ability of MBAseq to detect low-abundance strains. However, this finding does not imply that PCR cloning is incapable of detecting low-abundance strains; rather,

it highlights the limitation of sequencing only a minute subset of clones in a diagnostic setting. In the PDRC diagnostic laboratory workflow for resolution of mixed ARV populations, only five clones are routinely sequenced per sample, however, to assess the depth of sequencing that is attainable when more clones are sequenced, we selected and sequenced 20 recombinant clones for sample 145549. Notably, in sample 145549, one σC contig (M_145549_2) had the lowest coverage (75X) among all MBAseq-detected contigs across all isolates, yet it was still recovered by PCR cloning. This finding suggests that the resolution of PCR cloning could potentially be improved by sequencing a larger number of clones; however, such an approach is unlikely to be practical for routine diagnostic workflows.

Our results also reveal a high degree of sequence concordance between counterpart contigs generated by both methods. Pairwise alignment of amino acid sequences of these counterparts showed that 38 out of 43 sequence pairs had 99–100% similarity. This high similarity is not surprising given that a minimum of 20X mean coverage was used to generate consensus sequences for MinION-derived contigs—a more stringent threshold than a previous study, which showed that 5X coverage is sufficient for accurate consensus generation in sequencing the S1 subunit of infectious bronchitis virus spike protein (28). Furthermore, recent evidence indicates that the R10.4.1 flow cell used in this study produces significantly more accurate results compared to the earlier R9.4.1 flow cells (36).

A major impediment to adopting newer sequencing technologies in routine diagnostic workflows is analyzing the vast amount of data produced. However, the iteration of ONT's software (MinKNOW software version 24.06.16) used in this study integrates base-calling, demultiplexing, and adapter trimming, greatly reducing the reliance on third-party software as required in earlier studies (Butt et al., 2021; Young et al., 2021). Moreover, data generated in this

study demonstrates that the remainder of the analysis can be conducted using easily accessible and user-friendly bioinformatics tools such as the graphical user interface (GUI)-based Geneious Prime software. However, the use of bioinformatics tools such as Kraken and Centrifuge for taxonomic classification of reads may be an essential component of sequencing protocols that work directly with clinical samples or rely on random-primed amplification of genetic material. Such approaches often yield a higher proportion of host-derived sequences compared to our study, which employed targeted RT-PCR amplification prior to MBAseq, thereby reducing host background.

In conclusion, this study demonstrates the utility of MBAseq as tool for the accurate identification of ARV subpopulations within field isolates. Compared to conventional PCR cloning followed by Sanger sequencing, MBAseq not only offers a comparable alternative for strain-level characterization but also provides significantly greater resolution in detecting the full spectrum of viral diversity present in clinical samples. This increased sensitivity enables the identification of low-abundance viral variants that may be missed by conventional methods. As such, MBAseq could prove invaluable for viral surveillance, outbreak investigation, vaccine field efficacy evaluation, and the broader study of ARV epidemiology.

Acknowledgement

I sincerely appreciate Kelsey Young, April Skipper, Erich Linneman, Vanessa Gauthiersloan, Nicholas Davis-fields and Amanda Greenway for their excellent technical assistance and significant contribution towards making this study possible, and Dr Amal Mouhamed for her expert review of this manuscript.

References

1. Montgomery RD, Boyle CR, Maslin WR, Magee DL. Attempts to reproduce a runting/stunting-type syndrome using infectious agents isolated from affected Mississippi broilers. *Avian Diseases.*80-92; 1997.

2. Awandkar SP, Moregaonkar SD, Manwar SJ, Kamdi BP, Kulkarni MB. Comparative investigations of infectious runting and stunting syndrome in vaccinated breeder chicks by inactivated reovirus and chicks from non-vaccinated breeders. *Iran J Vet Res.* 18:6-12; 2017.

3. Yu H, Zhu Y, Wu Q, Zhao W, Wang Y, Wang D, Lu H, Diao Y, Li Y, Tang Y. Pathogenicity of avian reovirus variant in the immune organs of broiler chicks. *Virus research.* 353:199538; 2025.

4. Mansour SM, ElBakrey RM, Orabi A, Ali H, Eid AA. Isolation and detection of avian reovirus from tenosynovitis and malabsorption affected broiler chickens with involvement of vertical transmission. *Journal of Virological Sciences.* 4:24-32; 2018.

5. Sterner F, Rosenberger J, Margolin A, Ruff MAd. In vitro and in vivo characterization of avian reoviruses. II. Clinical evaluation of chickens infected with two avian reovirus pathotypes. *Avian Diseases.*545-554; 1989.

6. Davis JF, Kulkarni A, Fletcher O. Myocarditis in 9- and 11-day-old broiler breeder chicks associated with a reovirus infection. *Avian Dis.* 56:786-90; 2012.

7. Jones RC. Avian reovirus infections. *Rev Sci Tech (International Office of Epizootics).* 19:614-625; 2000.

8. Ayalew LE, Ahmed KA, Popowich S, Lockerbie BC, Gupta A, Tikoo SK, Ojkic D, Gomis S. Virulence of emerging arthrotropic avian reoviruses correlates with their ability to activate and

traffic interferon-gamma producing cytotoxic CD8(+) T cells into gastrocnemius tendon. *Front Microbiol.* 13:869164; 2022.

9. Ngunjiri JM, Ghorbani A, Jang H, Waliullah S, Elaish M, Abundo MC, Mahesh KC, Taylor KJ, Porter RE, Lee CW. Specific-pathogen-free turkey model for reoviral arthritis. *Vet Microbiol.* 235:170-179; 2019.

10. Walker ER, Friedman M, Olson N. Electron microscopic study of an avian reovirus that causes arthritis. *Journal of ultrastructure research.* 41:67-79; 1972.

11. Roessler DE, Rosenberger JK. In vitro and in vivo characterization of avian reoviruses. III. Host factors affecting virulence and persistence. *Avian Diseases.* 33:555-565; 1989.

12. Sellers HS. Current limitations in control of viral arthritis and tenosynovitis caused by avian reoviruses in commercial poultry. *Vet Microbiol.* 206:152-156; 2017.

13. French D. Incidence and economic impact of reovirus in the poultry industries in the United States. *Avian Diseases.* 66:432-434; 2022.

14. Goldenberg D. Avian reovirus in Israel, variants and vaccines—A review. *Avian Diseases.* 66:447-451; 2022.

15. Gamble T, Sellers H. Field control of avian reoviruses in commercial broiler production. *Avian Diseases.* 66:427-431; 2022.

16. Kant A, Balk F, Born L, Van Roozelaar D, Heijmans J, Gielkens A, Ter Huurne A. Classification of Dutch and German avian reoviruses by sequencing the sigma-C protein. *Veterinary research.* 34:203-212; 2003.

17. Troxler S, Rigomier P, Bilic I, Liebhart D, Prokofieva I, Robineau B, Hess M. Identification of a new reovirus causing substantial losses in broiler production in France, despite routine vaccination of breeders. *Veterinary Record.* 172:556-+; 2013.

18. Goldenberg D, Pasmanik-Chor M, Pirak M, Kass N, Lublin A, Yeheskel A, Heller D, Pitcovski J. Genetic and antigenic characterization of sigma C protein from avian reovirus. *Avian Pathol.* 39:189-99; 2010.

19. De Carli S, Wolf JM, Gräf T, Lehmann FK, Fonseca AS, Canal CW, Lunge VR, Ikuta N. Genotypic characterization and molecular evolution of avian reovirus in poultry flocks from Brazil. *Avian Pathology.* 49:611-620; 2020.

20. Jiang XN, Lin Y, Yang J, Wang HZ, Li C, Teng XY, Tang Y, Diao YX. Genetic characterization and pathogenicity of a divergent broiler-origin orthoreovirus causing arthritis in China. *Transbound Emerg Dis.* 00:1-11; 2020.

21. Mayahi M, Boroomand Z, Jafari RA, Khademian S, Hoseini H. Molecular identification of reovirus in broiler type flocks in Golestan province, Iran. *Iran J Vet Res.* 20:105-111; 2019.

22. Palomino-Tapia V, Mitevski D, Inglis T, van der Meer F, Abdul-Careem MF. Molecular characterization of emerging avian reovirus variants isolated from viral arthritis cases in Western Canada 2012-2017 based on partial sigma (sigma)C gene. *Virology.* 522:138-146; 2018.

23. Ayalew LE, Ahmed KA, Mekuria ZH, Lockerbie B, Popowich S, Tikoo SK, Ojkic D, Gomis S. The dynamics of molecular evolution of emerging avian reoviruses through accumulation of point mutations and genetic re-assortment. *Virus Evol.* 6: English. 2020.

24. Sellers HS. Avian reoviruses from clinical cases of tenosynovitis: An overview of diagnostic approaches and 10-year review of isolations and genetic characterization. *Avian Diseases.* 66:420-426; 2022.

25. Zhang T, Li H, Ma S, Cao J, Liao H, Huang Q, Chen W. The newest Oxford Nanopore R10.4.1 full-length 16S rRNA sequencing enables the accurate resolution of species-level microbial community profiling. *Applied and Environmental Microbiology.* 89:e00605-23; 2023.

26. Guo Y, Li Z, Li L, Li S, Sun L, Yang X, Dai Y, Gu J, Yang L, Liu X. A dual-process of targeted and unbiased Nanopore sequencing enables accurate and rapid diagnosis of lower respiratory infections. *EBioMedicine.* 98:104858; 2023.

27. Brown E, Freimanis G, Shaw AE, Horton DL, Gubbins S, King D. Characterising foot-and-mouth disease virus in clinical samples using nanopore sequencing. *Front Vet Sci.* 8:656256; 2021.

28. Butt SL, Erwood EC, Zhang J, Sellers HS, Young K, Lahmers KK, Stanton JB. Real-time, MinION-based, amplicon sequencing for lineage typing of infectious bronchitis virus from upper respiratory samples. *J Vet Diagn Invest.* 33:179-190; 2021.

29. Young KT, Lahmers KK, Sellers HS, Stallknecht DE, Poulson RL, Saliki JT, Tompkins SM, Padykula I, Siepker C, Howerth EW. Randomly primed, strand-switching, MinION-based sequencing for the detection and characterization of cultured RNA viruses. *J Vet Diagn Invest.* 33:202-215; 2021.

30. Spatz S, Afonso CL. Non-targeted RNA sequencing: towards the development of universal clinical diagnosis methods for human and veterinary infectious diseases. *Vet Sci.* 11:239; 2024.

31. Butt SL, Kariithi HM, Volkening JD, Taylor TL, Leyson C, Pantin-Jackwood M, Suarez DL, Stanton JB, Afonso CL. Comparable outcomes from long and short read random sequencing of total RNA for detection of pathogens in chicken respiratory samples. *Front Vet Sci.* 9:1073919; 2022.

32. Tang H, Han D. Rapid high-throughput sequencing: a game-changer for timely addressing infectious diseases. *EBioMedicine.* 114:105639; 2025.

33. Ji C-M, Feng X-Y, Huang Y-W, Chen R-A. The applications of nanopore sequencing technology in animal and human virus research. *Viruses.* 16:798; 2024.

34. Jain M, Olsen HE, Paten B, Akeson M. The Oxford Nanopore MinION: delivery of nanopore sequencing to the genomics community. *Genome biology.* 17:1-11; 2016.

35. Hoenen T. Sequencing of ebola virus genomes using nanopore technology. *Bio-protocol.* 6:e1998-e1998; 2016.

36. Ratcliff JD, Merritt B, Gooden H, Siegers JY, Srikanth A, Yann S, Kol S, Sin S, Tok S, Karlsson EA. Improved resolution of avian influenza virus using Oxford Nanopore R10 sequencing chemistry. *Microbiology Spectrum.* 12:e01880-24; 2024.

37. Croville G, Walch M, Sécula A, Lèbre L, Silva S, Filaire F, Guerin J-L. An amplicon-based nanopore sequencing workflow for rapid tracking of avian influenza outbreaks, France, 2020-2022. *Frontiers in Cellular and Infection Microbiology.* 14:1257586; 2024.

38. Spatz SJ, Garcia M, Riblet S, Ross TA, Volkening JD, Taylor TL, Kim T, Afonso CL. MinION sequencing to genotype US strains of infectious laryngotracheitis virus. *Avian Pathology.* 48:255-269; 2019.

39. Butt SL, Taylor TL, Volkening JD, Dimitrov KM, Williams-Coplin D, Lahmers KK, Miller PJ, Rana AM, Suarez DL, Afonso CL. Rapid virulence prediction and identification of Newcastle disease virus genotypes using third-generation sequencing. *Virol J.* 15:1-14; 2018.

40. da Silva AP, Aston EJ, Chiwanga GH, Birakos A, Muhairwa AP, Kayang BB, Kelly T, Zhou H, Gallardo RA. Molecular characterization of Newcastle disease viruses isolated from chickens in Tanzania and Ghana. *Viruses.* 12:916; 2020.

41. Edgar R. Muscle5: high-accuracy alignment ensembles enable unbiased assessments of sequence homology and phylogeny. Nat Commun 13: 6968. *Nature Communications.* 13:6968; 2022.

42. Narvaez SA, Harrell TL, Oluwayinka O, Sellers HS, Khalid Z, Hauck R, Chowdhury EU, Conrad SJ. Optimizing the conditions for whole-genome sequencing of avian reoviruses. *Viruses.* 15:1938; 2023.

Table 3. 1: Field isolates analyzed in this study and their tissue of origin

Sample 1D	Tissue of Origin
147334[A]	Tendon
148029[A]	Intestine
148785[A]	Tendon
149064[A]	Tendon
145549[B]	Vaccine
148512 [B]	Tendon
148784 [B]	Tendon
148807 [B]	Tendon
148845 [B]	Tendon
148847 [B]	Tendon
149107 [B]	Tendon
149127 [B]	Tendon
149132 [B]	Tendon
149220 [B]	Intestine
149222 [B]	Intestine
149223 [B]	Intestine
149230 [B]	Intestine
149715 [B]	Tendon
149720 [B]	Tendon
151882 [B]	Tendon
151883 [B]	Tendon
151886 [B]	Tendon
151890 [B]	Tendon
153142 [B]	Tendon

[A]Samples not to contain mixed populations after initial diagnostic sequencing

[B]Samples suspected to contain mixed populations after initial diagnostic sequencing

Table 3. 2 Heatmap of Amino Acid Similarity for Counterpart σC Contigs from MBAseq and PCR Cloning.

MBAseq	Similarity (%)	PCR C and Sanger Sequencing
M_145549_1	100	C_145549_1
M_145549_2	99.7	C_145549_2
M_145549_3	99.1	C_145549_3
M_148512_1	99.7	C_148512_1
M_148512_2	97.5	C_148512_2
M_148512_3	99.7	C_148512_3
M_148784_1	99.7	C_148784_1
M_148784_2	98.8	C_148784_2
M_148807_1	99.4	C_148807_1
M_148807_2	94.7	C_148807_2
M_148845_1	99.7	C_148845_1
M_148845_2	100	C_148845_2
M_148847_1	100	C_148847_1
M_148847_2	100	C_148847_2
M_149107_1	100	C_149107_1
M_149107_2	100	C_149107_2
M_149127_1	100	C_149127_1
M_149127_2	99.7	C_149127_2
M_149127_3	99.4	C_149127_3
M_149132_1	100	C_149132_1
M_149132_2	99.4	C_149132_2
M_149220_1	100	C_149220_1
M_149222_1	100	C_149222_1
M_149222_2	100	C_149222_2
M_149223_1	96.3	C_149223_1
M_149223_2	99.4	C_149223_2
M_149230_1	100	C_149230_1
M_149230_2	99.4	C_149230_2
M_149715_1	99.3	C_149715_1
M_149715_2	99.4	C_149715_2
M_149715_3	98.7	C_149715_3
M_149720_1	100	C_149720_1

M_151882_1	99.7	C_151882_1
M_151882_2	100	C_151882_2
M_151883_1	100	C_151883_1
M_151883_2	99.7	C_151883_2
M_151886_1	100	C_151886_1
M_151886_2	100	C_151886_2
M_151890_1	99.7	C_151890_1
M_151890_2	100	C_151890_2
M_151890_3	100	C_151890_3
M_153142_1	100	C_153142_1
M_153142_2	99.1	C_153142_2

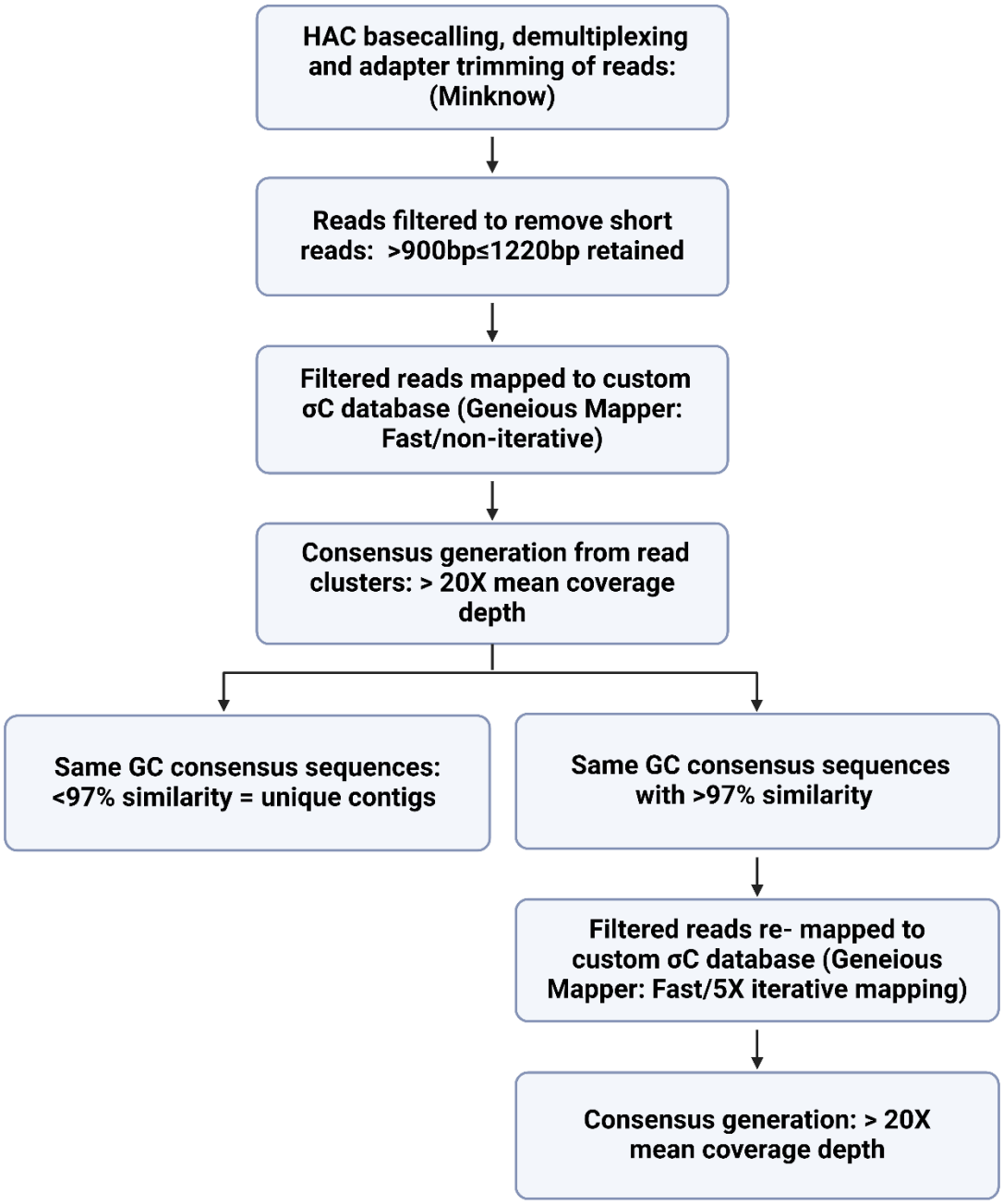

Figure 3. 1: A schematic diagram of the workflow for MinION-based amplicon sequencing (MBAseq) data analysis

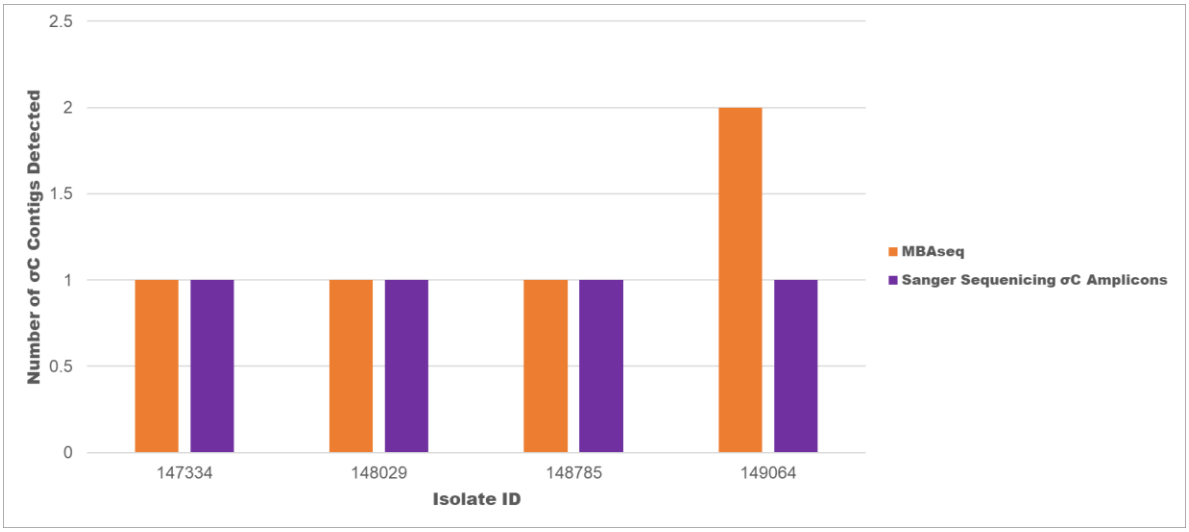

Figure 3.2: Summary of σC contigs identified by MBAseq and initial diagnostic Sanger sequencing of σC amplicons in isolates not suspected of harboring mixed ARV populations. Orange bars represent contigs identified by MBAseq, while purple bars indicate those identified by PCR cloning.

Figure 3.3: Summary of σC contigs identified by MBAseq and PCR cloning with Sanger sequencing in isolates containing heterogenous ARV populations. MBAseq contig counts are represented by orange bars, while PCR cloning and Sanger sequencing counts are shown as green bars.

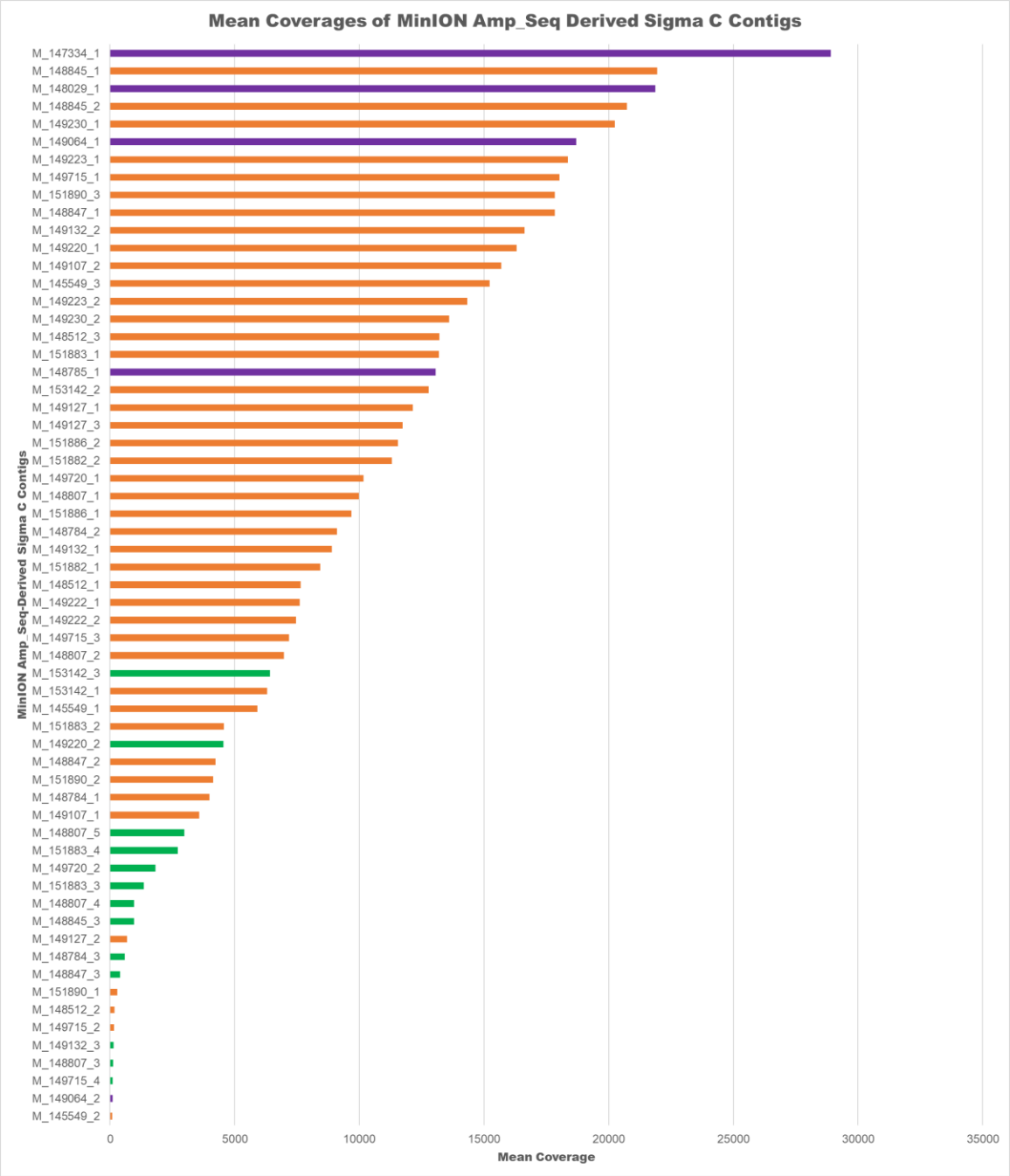

Figure 3.4: Mean coverages of MBAseq-derived σC contigs plotted in ascending order. Orange bars indicate contigs with PCR cloning counterparts, green bars represent contigs without PCR cloning counterparts, and purple bars denote contigs from samples determined not to contain mixed ARV populations at initial screening.

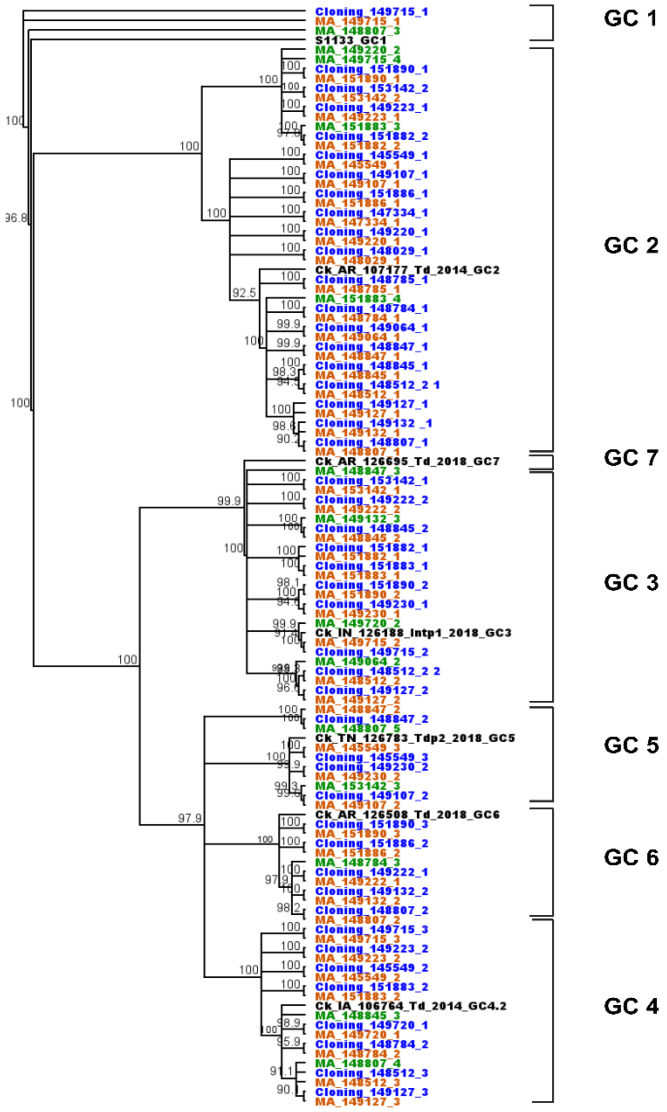

Figure 3. 5: Phylogenetic analysis of 115 partial σC sequences (310 amino acids), including 48 counterpart contig pairs from MBAseq (orange) and PCR cloning or amplicon Sanger sequencing (blue). Green-labeled contigs represent 14 MBAseq-derived sequences without corresponding counterparts. Black-labeled references denote all known ARV genetic clusters (GCs). Multiple sequence alignment and phylogenetic tree construction were performed in Geneious Prime 2024.0.5 using Clustal Omega and the neighbor-joining method with 1,000.

CHAPTER 4

WHOLE-GENOME AND SINGLE-PREDICTED PROTEIN PHYLOGENETIC ANALYSIS OF AVIAN REOVIRUS FIELD ISOLATES[1]

[1] **Oluwayinka, Olatunde and [1]Holly S. Sellers.** To be submitted to *Avian Diseases.*

Keywords: Avian reovirus, next generation sequencing, whole genome sequencing, phylogeny

Abbreviations: ARV – Avian reovirus; DNA – Deoxyribonucleic acid; GC – Genotypic cluster; PDRC – Poultry Diagnostic and Research Center; RNA – Ribonucleic acid; RT-PCR – Reverse transcriptase polymerase chain reaction

Summary

Avian reoviruses (ARVs) are associated with various diseases in poultry such as arthritis, tenosynovitis, and immunosuppression, resulting in significant economic losses in the U.S. and worldwide due to reduced productivity, increased mortality, and costs of vaccination and control. ARVs belong to the genus *Orthoreovirus* and possess a 10-segment double-stranded RNA genome encoding eight structural and four nonstructural proteins. To date, seven genotypic clusters (GCs) have been defined based on sequence variation in the minor outer capsid protein, σC.

This study aimed to characterize the genetic diversity and evolutionary relationships among ARV field strains by reconstructing phylogenies based on the full predicted viral proteome and individual proteins, and comparing these phylogenies with the σC-based phylogeny.

Twelve ARV field isolates representing GC1, GC2, GC5, GC6, and GC7 were sequenced using Illumina paired-end technology. All ten genomic segments were successfully assembled per isolate. Amino acid sequences from all predicted coding regions were used to construct proteome-wide and segment-specific phylogenies using the neighbor-joining method with the Jukes-Cantor model and 1,000 bootstrap replicates.

Findings revealed that predicted proteome-based phylogeny was largely congruent with σC-based clustering, highlighting the strong diversifying role σC and its reflection of overall ARV evolution. Compared to σC, other S1-encoded proteins (p10, p17) also showed high variability and had phylogenies that clustered according to σC-defined GCs, suggesting likely co-evolution of S1-encoded proteins. Among M-class proteins, μB was the most variable and and showed phylogenetic incongruence with σC suggesting that although both are surface proteins, μB is likely subject to distinct evolutionary pressures and thus follows a different evolutionary path compared to σC. The vaccine strain S1133 grouped differently in λC, σB, and σNS phylogenies this could

indicate that changes in these proteins may be associated with attenuation. In addition, isolates 127720 and 126695 represent the first full-genome sequences reported for GC7. Strain 127720 displayed marked divergence in σA, an otherwise conserved protein, highlighting its potential evolutionary significance.

In conclusion, this study enhances understanding of ARV genetic diversity, the evolutionary significance of S1 proteins, highlights ARV proteins that are likely associated with attenuation based on Sigma C divergence in specific viral proteins phylogeny.

Introduction

Avian reovirus (ARV) continues to challenge poultry health by causing arthritis/tenosynovitis outbreaks that result in lameness, stunted growth, and significant economic losses (1). Despite widespread vaccination, emerging ARV variants appear to evade immune protection, underscoring the need for a deeper understanding of viral evolution (2, 3). ARV is a segmented, non-enveloped dsRNA virus whose genomic segments are named based on their electrophoretic mobility, viz: large (L1-L3), medium (M1-M3) and small (S1-S4). This genome encodes 8 structural proteins (λA, λB, λC, μA, μB, σA, σB, and σC,) and 4 nonstructural proteins (μNS, σNS, p10 and p17) (4). The L segments encode core proteins involved in scaffolding (λC), transcription (λB) and capping (λC), the M segments encode proteins essential for viral entry and outer capsid formation (μB), and formation of viral factories (μNS). The S1 segment is tricistronic encoding the highly variable σC protein, along with p10 (nonstructural fusogenic protein) and p17 (nonstructural nuclear protein) while S2, S3 and S4 encode 2 structural (σA and σB) and one nonstructural protein (σNS). σC is pivotal for host cell attachment and serves as a key target of host neutralizing antibody (5). Sequence of σC has been used for characterization of ARV isolates with 7 GCs identified at the present (3). A major limitation of σC-based phylogeny is that it provides limited information in relation to the pathobiology of ARV isolates.

Previous studies have documented extensive genetic diversity in ARV, with reports of significant reassortment events and point mutations driving its evolution (6-10). These findings highlight the complex interplay between viral evolution and vaccine efficacy, as emerging variants often escape immune responses elicited by current vaccines.

In the present study, we employed deep next-generation sequencing to comprehensively characterize ARV field isolates representing GCs 1, 2,5, 6 and 7. Evolutionary relationships were

assessed using the neighbor-joining method with the Jukes-Cantor model and 1,000 bootstrap replicates—a robust and computationally efficient approach well-suited for large datasets (11). Our analyses involved both concatenated amino acid sequences from all viral proteins and individual protein sequences. A primary objective was to compare the whole-genome phylogeny and protein-specific phylogenies with the established σC-based phylogeny, thereby evaluating the extent to which the latter reflects overall viral evolution.

Materials and Methods

Viruses. Twelve plaque purified ARV isolates provided by the Poultry Diagnostic and Research Center (PDRC) were analyzed in this study. As part of the initial diagnostic workup, the isolates were molecularly characterized by RT-PCR amplification and sequencing of the genomic region encoding the σC protein. Based on this analysis, four isolates were classified as GC1, one as GC2, three as GC5, and two each as GC6 and GC7 (Table 4. 1). Upon receipt, virus stocks were aliquoted and stored at –80°C for subsequent analyses.

Virion purification, nuclease treatments, RNA extraction and depletion of host genetic material. Seven of 12 plaque purified ARV stocks (Table 4. 1) were processed as previously described (12). Briefly, each virus stock was mixed with Capto Core 700 slurry (Cytiva, Marlborough, MA, USA) and purified through two rounds of incubation and centrifugation (800 × g for 10 minutes). The supernatant was then further clarified using an Illustra MicroSpin column (Cytiva, Marlborough, MA, USA) at 800 × g for 5 minutes. RNA was extracted from 350 µL of the purified sample using the MagMAX Viral RNA Isolation Kit (Thermo Fisher Scientific, Waltham, MA, USA), following the manufacturer's protocol. Extracted RNA was aliquoted and stored at –80 °C until further use.

Subsequently, host and bacterial ribosomal RNA (rRNA) were depleted using custom single-stranded DNA probes (Integrated DNA Technologies, Coralville, IA, USA) that hybridized to host and bacterial RNA in a PCR-like reaction, followed by RNase H treatment (New England Biolabs, Ipswich, MA, USA) to digest probe-bound RNA (13). The rRNA-depleted RNA was further purified using RNAClean XP beads (Beckman Coulter, Brea, CA, USA) at a 2.2X ratio and quantified using the Agilent 2100 Bioanalyzer (Agilent Technologies, Santa Clara, CA, USA).

For the remaining five viral stocks, total RNA was extracted using the Quick-RNA Viral Kit (Zymo Research, Irvine, CA, USA). RNA concentration was measured with a NanoDrop 2000 spectrophotometer (Thermo Fisher Scientific, Waltham, MA, USA). All RNA samples were aliquoted and stored at –80 °C until further use.

cDNA synthesis and PCR amplification. The single primer amplification protocol (R-SPA) described by Chrzastek et al. (14) was used to generate ARV cDNA for whole-genome sequencing. Briefly, 10 µL of ARV RNA was mixed with 1 µL of 100 µM primer R8N, 1 µL of 10 mM dNTPs, and 1 µL nuclease-free water, then incubated at 95°C for 4 min and chilled on ice. This mix was combined with 7 µL of a SuperScript IV reaction mix (containing 4 µL of 5X buffer, 1 µL of 100 mM DTT, 1 µL RNaseOUT, and 1 µL SuperScript IV reverse transcriptase), and incubated sequentially at 23°C (10 min), 55°C (10 min), and 80°C (10 min). Second-strand synthesis was carried out immediately by adding 1 µL of primer 10 MR8N, 1 µL of 10 mM dNTPs, and 2 µL of 10X Reaction Buffer to the cDNA, followed by incubation at 94°C for 3 min, cooling to 4°C, and then addition of 1 µL Klenow polymerase with incubation at 37°C for 60 min. The resulting double-stranded cDNA was purified using 1.8X AMPure XP beads and subsequently amplified using the HiFi PCR Phusion kit under the following conditions: initial denaturation at 98°C for 30 s; 35 cycles of 98°C for 30 s, 50°C for 30 s, and 72°C for 1 min; with a final extension

at 72°C for 10 min. The final PCR products were purified again using 1.8X AMPure XP beads. Amplified products were converted into sequencing libraries for Illumina sequencing, which was performed at either the U.S. National Poultry Research Center (USNPRC) in Athens, GA, or at SeqCenter in Pittsburgh, PA (Table 4.1)

Whole Genome Sequencing. USNPRC sequencing: Genomic libraries were generated for six viruses with the Nextera XT DNA Library Preparation Kit (Illumina, San Diego, CA, USA) and IDT for Illumina DNA/RNA UD Indexes Set A (Illumina, San Diego, CA, USA). Samples were run using a MiSeq Reagent Nano Kit v2 500 cycles cartridge (Illumina, San Diego, CA, USA) on an Illumina Miseq instrument (Illumina, San Diego, CA, USA).

SeqCenter sequencing**:** Illumina sequencing libraries were prepared for six viruses using the tagmentation-based and PCR-based Illumina DNA Prep kit (Illumina, San Diego, CA, USA) and custom IDT 10bp unique dual indices (UDI) with a target insert size of 280 bp. No additional DNA fragmentation or size selection steps were performed. Illumina sequencing was performed on an Illumina NovaSeq X Plus sequencer in one or more multiplexed shared-flow-cell runs, producing 2x151bp paired-end reads.

Bioinformatics analysis of sequencing reads. Raw sequencing reads were trimmed and filtered using Trimmomatic (15). retaining reads with Phred scores >30. Filtered reads were mapped to the chicken reference genome (NCBI accession: GCF_016699485.2) using the BWA aligner (16) Unmapped reads, presumed to contain viral sequences, were extracted using SAMtools v1.16.1(17) . and subsequently classified taxonomically with Kraken 2 (18) to estimate the proportion of ARV reads in each sample. When the estimated number of ARV reads exceeded that required for 100× genome coverage, a representative subset was extracted using Seqtk Toolkit (19). If the number of ARV reads was insufficient, all unmapped reads were retained. Selected

reads were then assembled de novo using SPAdes v3.15.3 (20). Resulting contigs were imported into Geneious Prime 2024.0.5 and queried against the NCBI nucleotide database using BLAST. ARV contigs were sorted into their respective genome segments. For segments that were fragmented or shorter than expected, a reference-guided assembly approach was adapted from Narvaez et al (12) In this step, closely matching reference sequences (identified via BLAST) were incorporated into a multifasta file. Reads were then mapped to this reference using BWA mem (16). The resulting BAM file was sorted and imported into Geneious Prime, where the alignments were visually inspected, and consensus sequences were generated for each segment.

Phylogenetic analysis of sequences. In addition to the ARV genomes sequenced in this study, two publicly available complete genomes—S1133 (KF741756–KF741765), a widely used vaccine strain belonging to GC 1, and AVS-B (FR694191–FR694200), a strain associated with runting-stunting syndrome and classified as GC 4 — were included for comparative analysis. Protein-coding sequences were extracted from each assembled genome and predicted amino acid sequences were generated in Geneious Prime.

Multiple sequence alignments were performed using MUSCLE v5 (21) for each individual protein as well as concatenated sequences representing the full viral proteome. Phylogenetic relationships were inferred using the neighbor-joining method with the Jukes-Cantor substitution model and 1,000 bootstrap replicates. Both complete genome alignments and individual protein-based alignments were used to assess topological congruence and segment-specific evolutionary signals.

Results

σC and Viral Proteome Phylogeny. All genomic segments of the twelve ARV field isolates were assembled from paired-end Illumina sequencing reads. To investigate viral proteome

and gene-specific phylogenies, predicted concatenated and individual amino acid sequences derived from the partial or complete coding regions of all twelve ARV proteins were analyzed. Phylogenetic relationships among isolates were inferred using the neighbor-joining method with the Jukes-Cantor model and 1,000 bootstrap replicates.

The tricistronic S1 segment encodes the proteins p10, p17, and σC. σC was highly divergent, with pairwise amino acid identities ranging from 49.1% to 99.4% (Table 4.2). The resulting σC phylogeny resolved six distinct GCs (GCs 1, 2, 4, 5, 6, and 7) (Fig. 4. 1A). Predicted whole proteome analysis of all 12 ARV proteins revealed overall pairwise identities ranging from 87.3% to 98.7%. The topology of the predicted proteome phylogenetic tree generally mirrored the σC-based clusters, indicating that σC evolution largely reflects broader viral evolutionary patterns. Minor deviations from σC phylogeny were noted including that GC6 and GC7 lineages may share a recent common ancestor (Fig. 4.1B).

Alignments and phylogeny of deduced amino acids sequences of L- class proteins. Analysis of predicted amino acid sequences for λA showed minimal variability (97.5–100% identity), while λB and λC were more divergent (95.6–99.8% and 83–99.7%, respectively) as shown in Table 4.2. Phylogenetic trees of L-class proteins (Fig. 4. 2) consistently placed GC1 variants 115940 and 117816 together, distinct from other GC1 strains. Inter-GC clustering was observed; for instance, strain 106761(GC 2) clustered with 126695 (GC7) in the λB phylogeny (Fig.4. 2B), and strain 122301 (GC6) was related to 115940 and 117816 (GC1) in the λC tree. Further, S1133 is clearly distant from other viruses in the λC phylogeny suggesting that the attenuation process likely induced changes in this protein (Fig. 4. 2C)

Alignments and phylogeny of deduced amino acids sequences of M- class proteins. The M1, M2, and M3 segments of ARV encode μA, μB, and μNS proteins, respectively. Among

these, as shown in Table 4.2, μB showed the highest variability (85–100% identity), compared to μA (94.9–99.7%) and μNS (89.9–99.7%). The phylogenies of M-class proteins (Fig. 4. 3) did not consistently align with the σC-based classification. In both μA (Fig. 4. 3A) and μNS (Fig. 3C) trees, S1133 appeared to represent separate cluster, whereas in the μB tree (Fig. 4.3B), it grouped with strains 94594 (GC5), 106761 (GC2), 122301 (GC6), and 126484 (GC1). GC1 variants 115940 and 117816 consistently clustered together across M-class phylogenies.

Alignments and phylogeny of deduced amino acids sequences of other S- class proteins. The other S1-encoded proteins, p10 and p17, also displayed high variability (70.7–100% and 53.4–100% identity (Table 4.2), respectively), and their phylogenies were congruent with σC-defined clusters. Within the GC1 lineage in both phylograms, similar to σC phylogeny, 96139, 126484 and S1133 likely represent sub-lineages (Fig. 4.4). In contrast, σA sequences were highly conserved (97.4–99.7% identity) (Table 4.2) except for isolate 127720 (GC7), which was distinctly divergent. The lack of bootstrap support for σA underscores its limited phylogenetic informativeness, though 127720 remained clearly separated (Fig 4.5A). Finally, σB and σNS exhibited 92.9–100% and 92.4–99.7% identities, respectively (Table 4.2), with phylogenetic trees that were incongruent with the σC topology (Table 4.5B & C). Notably, S1133 appeared more evolutionarily distant in both σB and σNS trees, suggesting that the process of attenuation may have induced significant changes.

Discussion and Conclusion

The comprehensive phylogenetic analysis of ARV field isolates conducted in this study reveals a complex evolutionary landscape. Whole-genome sequencing and phylogenetic reconstruction based on concatenated amino acid sequences from all 12 ARV proteins demonstrated that overall evolutionary relationships among isolates largely align with σC-defined

genotypic clusters. This observation contrasts with a previous study (4) which reported incongruence between whole-genome and σC-based phylogenies.

These differing outcomes are likely attributable to variations in the methods utilized. In the present study, amino acid sequences from predicted protein-coding regions were used, rather than nucleotide sequences. This approach enabled accurate resolution of all three partially overlapping open reading frames (ORFs) within the S1 segment—namely, p10, p17, and σC. Consequently, the evolutionary signals from p10 and p17, which exhibited phylogenetic topologies similar to that of σC, were incorporated into the whole-proteome phylogeny. In contrast, analyses based on S1 nucleotide sequences without resolving overlapping ORFs risk excluding these contributions, potentially obscuring true evolutionary relationships. In addition, this finding supports the report from an earlier study that the S1 segment contains more nonsynonymous amino acid changes compared to other segments of the virus(6) .

The commercial vaccine strain S1133 appears evolutionarily distinct from other viruses across all phylogenies, except for those based on the predicted amino acid sequences of S1-encoded and μB proteins. This suggests that, although S1133 is widely used as a live attenuated vaccine, it likely does not participate in reassortment events. In contrast, other GC1 variants (96139, 126484) with the exception of isolates 115940 and 117816 cluster with viruses from different GCs in multiple trees (λB, μA, μB, and μNS) . On the other hand, GC1 isolates 115940 and 117816 consistently cluster together in all phylogenies and changes between them are few, suggesting that point mutation rather that reassortment may drive changes between these viruses.

For the L -class phylogeny, λA exhibited high conservation, λB and λC displayed considerable variability, with S1133 contributing to marked divergence in λC. There is evidence of inter-genotypic clustering such as the clustering of strain 106761 (GC 2) with GC7 strain

126695 in the λB phylogeny and the evolutionary relationship of strain 122301 (GC6) with GC1 variants 115940 and 117816 in the λB tree.

The analysis of M-class proteins revealed that μB is notably more variable than μA and μNS, (Table 4.2) and being the major capsid protein (4, 22, 23), this may reflect its role as a target for host immune responses.

In the S-class, the high divergence of Sigma C is well documented (3, 24), and our findings confirm this with pairwise identities ranging from as low as 49.1% to 99.4%, leading to the delineation of six distinct clusters. Other S1 proteins also showed considerable diversities with pairwise identities ranging from 70.7–100% for p10 and 53.4–100% p17. However, the congruence observed among the phylograms of S1 proteins is inconsistent with the findings of previous studies (6, 7).Further, within the S-class proteins σA lies at the other end of the sequence diversity spectrum, being highly conserved. The phylogram of σA proved to be phylogenetically uninformative for resolving relationships among isolates, aside from clearly distinguishing the divergent strain 127720 (GC 7).

Two GC7 strains—127720 and 126695—were sequenced in this study, representing, to our knowledge, the first whole-genome sequences reported for viruses in this GC. A particularly striking observation in GC7 was the divergent σA protein found in strain 127720. The σA protein functions as a viral dsRNA binding protein (25) and is it also been established to be associated with interferon resistance among ARV infections (26). It remains unclear whether the divergence observed in 127720's σA confers an evolutionary advantage, considering that GC7 variants were only recovered from clinical samples between 2017 and 2018 and have not been reported subsequently. Importantly, this divergence was not observed for strain 126695, suggesting that it is not a common feature among GC7 isolates.

Overall, these results underscore the significance of the σC protein in the phylogeny of ARV and suggest two potential directions for developing a new molecular typing scheme. One possibility is that σC is indispensable for any robust ARV phylogeny, serving as a critical marker for distinguishing strains. Alternatively, the pronounced diversifying influence of σC may obscure the evolutionary signals of other viral proteins, indicating that its inclusion could skew phylogenetic analyses. In this case, it might be advantageous either to exclude σC or to mitigate its influence, for example, by using a truncated version of the protein.

Finally, the observed genetic variability, evidence of point mutation and reassortment events carry significant implications for vaccine design and epidemiological surveillance. As ARV continues to evolve, comprehensive genomic analyses will remain to be crucial for monitoring emerging strains and informing effective control strategies in poultry production.

Acknowledgement

I sincerely appreciate Drs. Sonsiray Alvarez-Narvaez and Telvin Harrell for their invaluable help with various aspects of Illumina Miseq sequencing, and Mr. Erich Linneman for his help at preparation and shipping of amplified viral segments for sequencing.

References

1. French D. Incidence and economic impact of reovirus in the poultry industries in the United States. *Avian Diseases.* 66:432-434; 2022.

2. Ayalew LE, Gupta A, Fricke J, Ahmed KA, Popowich S, Lockerbie B, Tikoo SK, Ojkic D, Gomis S. Phenotypic, genotypic and antigenic characterization of emerging avian reoviruses isolated from clinical cases of arthritis in broilers in Saskatchewan, Canada. *Sci Rep-Uk.* 7: English. 2017.

3. Sellers HS. Avian reoviruses from clinical cases of tenosynovitis: An overview of diagnostic approaches and 10-year review of isolations and genetic characterization. *Avian Diseases.* 66:420-426; 2022.

4. Benavente J, Martínez-Costas J. Avian reovirus: structure and biology. *Virus research.* 123:105-119; 2007.

5. Dawe WH, Kapczynski DR, Linnemann EG, Gauthiersloan VR, Sellers HS. Analysis of the Immune Response and Identification of Antibody Epitopes Against the Sigma C Protein of Avian Orthoreovirus Following Immunization with Live or Inactivated Vaccines. *Avian Diseases.* 66:465 - 475; 2022.

6. Ayalew LE, Ahmed KA, Mekuria ZH, Lockerbie B, Popowich S, Tikoo SK, Ojkic D, Gomis S. The dynamics of molecular evolution of emerging avian reoviruses through accumulation of point mutations and genetic re-assortment. *Virus Evol.* 6: English. 2020.

7. Teng L, Xie Z, Xie L, Liu J, Pang Y, Deng X, Xie Z, Fan Q, Luo S, Feng J. Sequencing and phylogenetic analysis of an avian reovirus genome. *Virus Genes.* 48:381-386; 2014.

8. Narvaez SA, Harrell TL, Day JM, Conrad SJ. Whole genome sequence analysis of turkey orthoreovirus isolates reveals a strong viral host-specificity and naturally occurring co-infections in commercial turkeys. *Virology.* 600:110216; 2024.

9. Nour I, Alvarez-Narvaez S, Harrell TL, Conrad SJ, Mohanty SK. Whole genomic constellation of avian reovirus strains isolated from broilers with arthritis in North Carolina, USA. *Viruses.* 15:2191; 2023.

10. Egana-Labrin S, Hauck R, Figueroa A, Stoute S, Shivaprasad HL, Crispo M, Corsiglia C, Zhou H, Kern C, Crossley B*, et al.* Genotypic Characterization of Emerging Avian Reovirus Genetic Variants in California. *Sci Rep-Uk.* 9: English. 2019.

11. Saitou N, Nei M. The neighbor-joining method: a new method for reconstructing phylogenetic trees. *Molecular biology and evolution.* 4:406-425; 1987.

12. Narvaez SA, Harrell TL, Oluwayinka O, Sellers HS, Khalid Z, Hauck R, Chowdhury EU, Conrad SJ. Optimizing the conditions for whole-genome sequencing of avian reoviruses. *Viruses.* 15:1938; 2023.

13. Parris DJ, Kariithi H, Suarez DL. Non-target RNA depletion strategy to improve sensitivity of next-generation sequencing for the detection of RNA viruses in poultry. *J Vet Diagn Invest.* 34:638-645; 2022.

14. Chrzastek K, Sellers HS, Kapczynski DR. A universal, single primer amplification protocol (R-SPA) to perform whole genome sequencing of segmented dsRNA reoviruses. *bioRxiv.*2021.11. 01.466778; 2021.

15. Bolger AM, Lohse M, Usadel B. Trimmomatic: a flexible trimmer for Illumina sequence data. *Bioinformatics.* 30:2114-2120; 2014.

16. Li H. Aligning sequence reads, clone sequences and assembly contigs with BWA-MEM. *arXiv preprint arXiv:1303.3997.* 2013.

17. Li H, Handsaker B, Wysoker A, Fennell T, Ruan J, Homer N, Marth G, Abecasis G, Durbin R, Subgroup GPDP. The sequence alignment/map format and SAMtools. *bioinformatics.* 25:2078-2079; 2009.

18. Wood DE, Lu J, Langmead B. Improved metagenomic analysis with Kraken 2. *Genome biology.* 20:1-13; 2019.

19. Li H. seqtk Toolkit for processing sequences in FASTA/Q formats. *GitHub.* 767:69; 2012.

20. Prjibelski A, Antipov D, Meleshko D, Lapidus A, Korobeynikov A. Using SPAdes de novo assembler. *Current protocols in bioinformatics.* 70:e102; 2020.

21. Edgar R. Muscle5: high-accuracy alignment ensembles enable unbiased assessments of sequence homology and phylogeny. Nat Commun 13: 6968. *Nature Communications.* 13:6968; 2022.

22. Huang DD, Nugent MA, Rosenberger JK, Schnitzer TJ. Association of avian reovirus M and S genes with viral behavior in vivo. I. Viral persistence. *Avian Diseases.* 31:438-445; Language of Summary: Spanish; Castilian. 1987.

23. Su YP, Su BS, Shien JH, Liu HJ, Lee LH. The sequence and phylogenetic analysis of avian reovirus genome segments M1, M2, and M3 encoding the minor core protein mu A, the major outer capsid protein mu B, and the nonstructural protein mu NS. *J Virol Methods.* 133:146-157; 2006.

24. Sellers HS. Current limitations in control of viral arthritis and tenosynovitis caused by avian reoviruses in commercial poultry. *Vet Microbiol.* 206:152-156; 2017.

25. Huang PH, Li YJ, Su YP, Lee LH, Liu HJ. Epitope mapping and functional analysis of sigma A and sigma NS proteins of avian reovirus. *Virology.* 332:584-595; 2005.

26. Gao L, Liu R, Luo D, Li K, Qi X, Liu C, Zhang Y, Cui H, Wang S, Gao Y. Avian reovirus Σa protein inhibits type I interferon production by abrogating interferon regulatory factor 7 activation. *J Virol.* 97:e01785-22; 2023.

Table 4. 1: Table of 12 plaque purified isolates sequenced in this study, including, their σC defined genotypic cluster, host, tissue of isolation and location of sample.

Isolate ID	Genetic Cluster	Host	Tissue of Origin	Location
115940[A]	GC 1	Chicken	Tendon	TX, USA
117816[A]	GC 1	Chicken	Tendon	TX, USA
126484[B]	GC 1	Chicken	Tendon	IA, USA
96139[B]	GC 1	Chicken	Tendon	GA, USA
106761[A]	GC 2	Chicken	Tendon	IA, USA
131930[B]	GC 5	Chicken	Tendon	GA, USA
94594[B]	GC 5	Chicken	Tendon	GA, USA
126963[A]	GC 5	Chicken	Tendon	PA, USA
143572[B]	GC 6	Chicken	Tendon	AR, USA
122301[A]	GC 6	Chicken	Tendon	AR, USA
127720[B]	GC 7	Chicken	Tendon	IA, USA
126695[A]	GC 7	Chicken	Tendon	AR, USA

[A]Isolates that did not undergo virion purification, were not subjected to host RNA depletion, and were sequenced at the SeqCenter, Pittsburg, PA

[B]Isolates that underwent virion purification, were subjected to host RNA depletion, and sequenced at the USNPRC, Athens, GA.

Table 4. 2: Summary of Pairwise Amino Acid Identity Ranges of Predicted ARV Individual Proteins and Whole Proteome

Viral Protein	% Pairwise Identity (Min–Max)
λA	97.5 -100%
λB	95.6 - 99.8%
λC	83 - 99.7%
μA	94.9 - 99.7%
μB	85 - 100%
μNS	89.9 - 99.7%
p10	70.7 - 100%
p17	53.4 - 100%
σC	49.1 99.4%
σA	97.4 - 99.7%[B]
σB	92.9 - 100%
σNS	92.4 -99.49
Whole Viral proteome	87.3 -98.7%

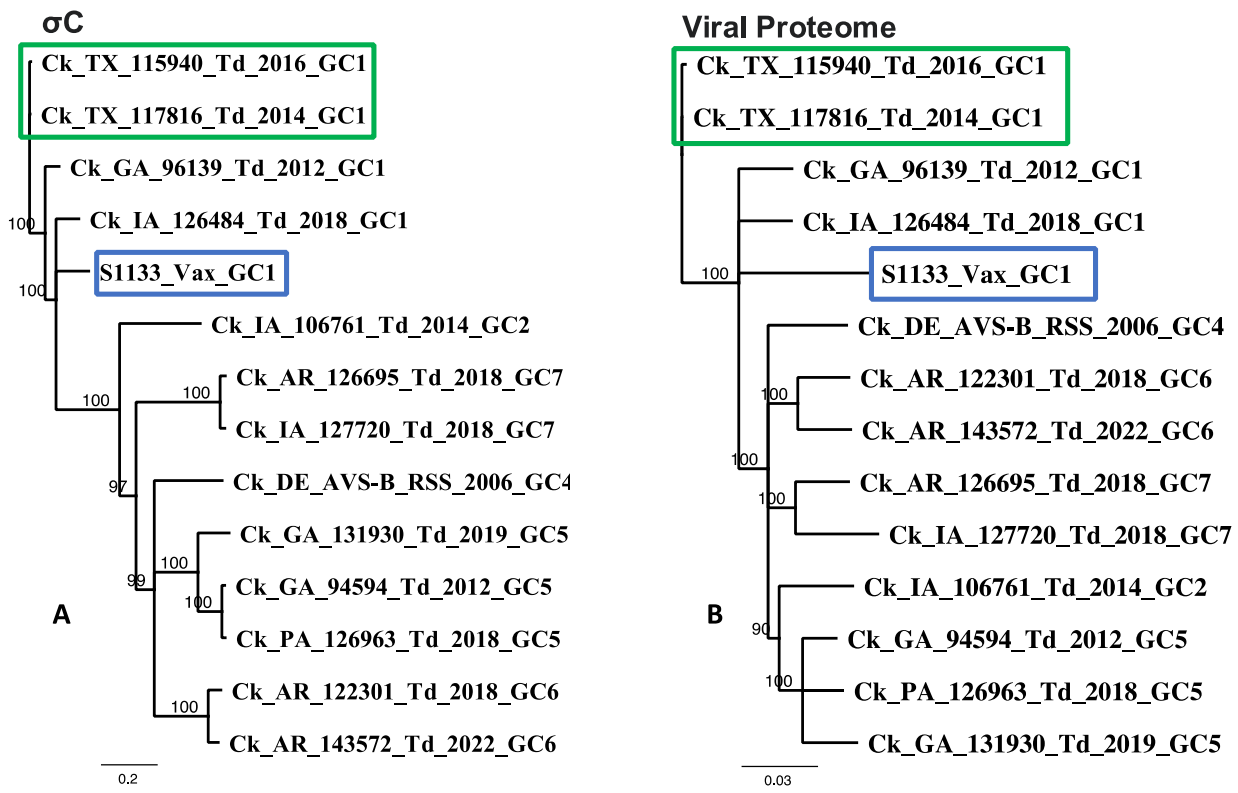

Fig. 4.1: Phylogenetic trees of ARV λA (A), λB (B) and λNS (C) protein. Field isolates sequenced in this study and strain AVS_B are named per convention proposed by Sellers, 2022 (3) and their specific GC is added to the end of their names. Green box delineates cluster that include GC1 variants 115940 and 117816 and blue box delineates S1133 vaccine strain

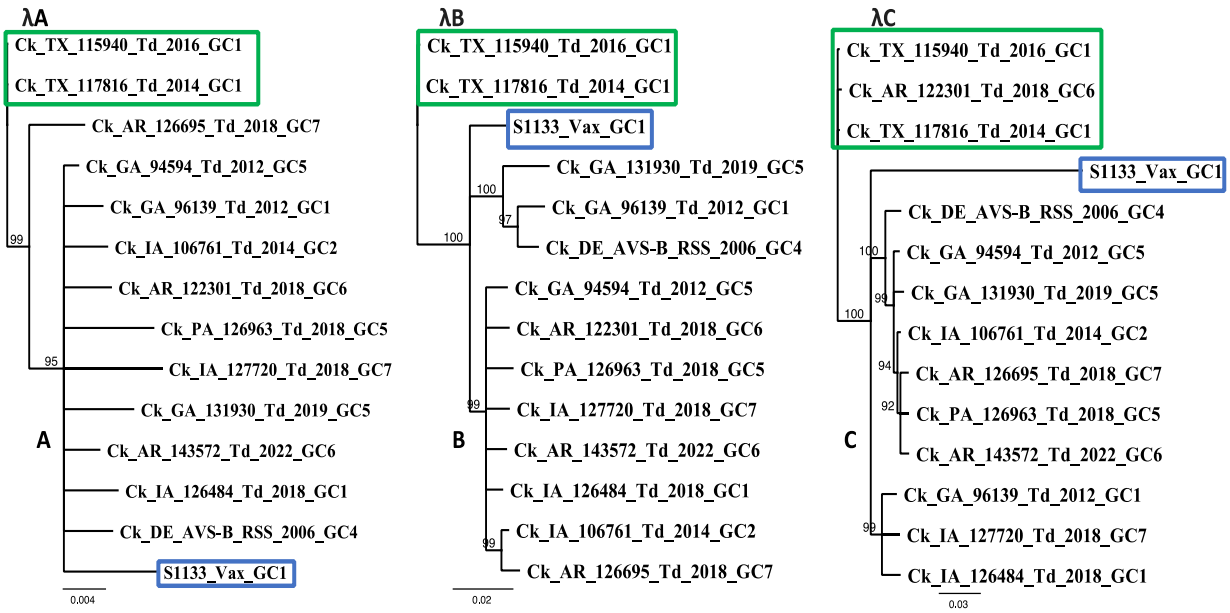

Figure 4.2: Phylogenetic trees of ARV λA (A), λB (B) and λNS (C) protein. Field isolates sequenced in this study and strain AVS_B are named per convention proposed by Sellers, 2022 (3) and their specific GC is added to the end of their names. Green box delineates cluster that include GC1 variants 115940 and 117816 and blue box delineates S1133 vaccine strain.

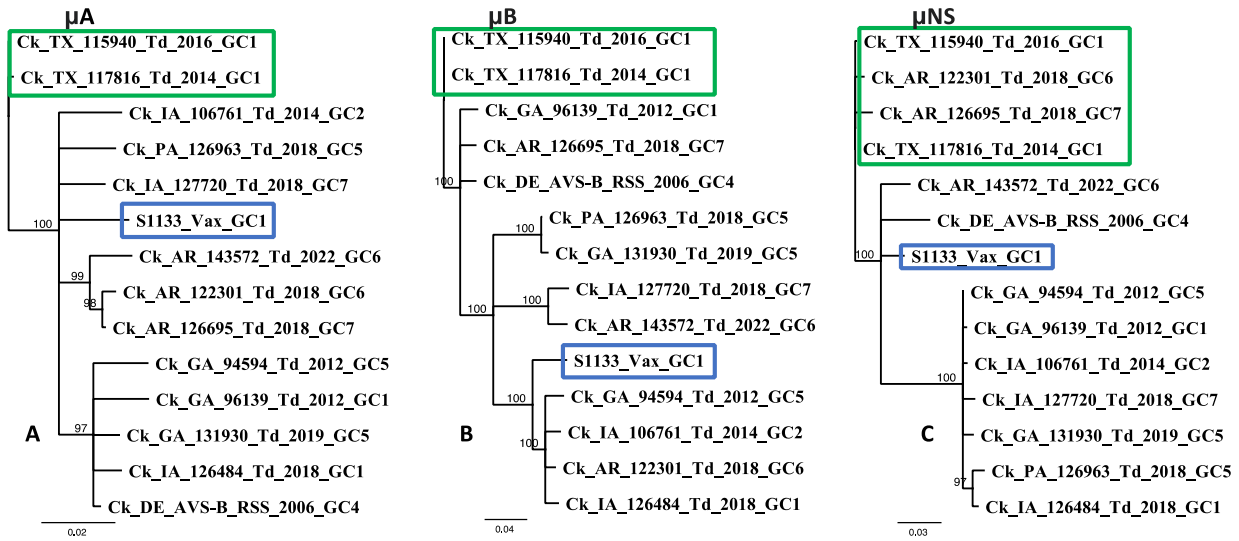

Fig. 4.3: Phylogenetic trees of ARV μA (A), μB (B) and μNS (C) protein. Field isolates sequenced in this study and strain AVS_B are named per convention proposed by Sellers, 2022 (3) and their specific GC is added to the end of their names. Green box delineates cluster that include GC1 variants 115940 and 117816 and blue box delineates S1133 vaccine strain.

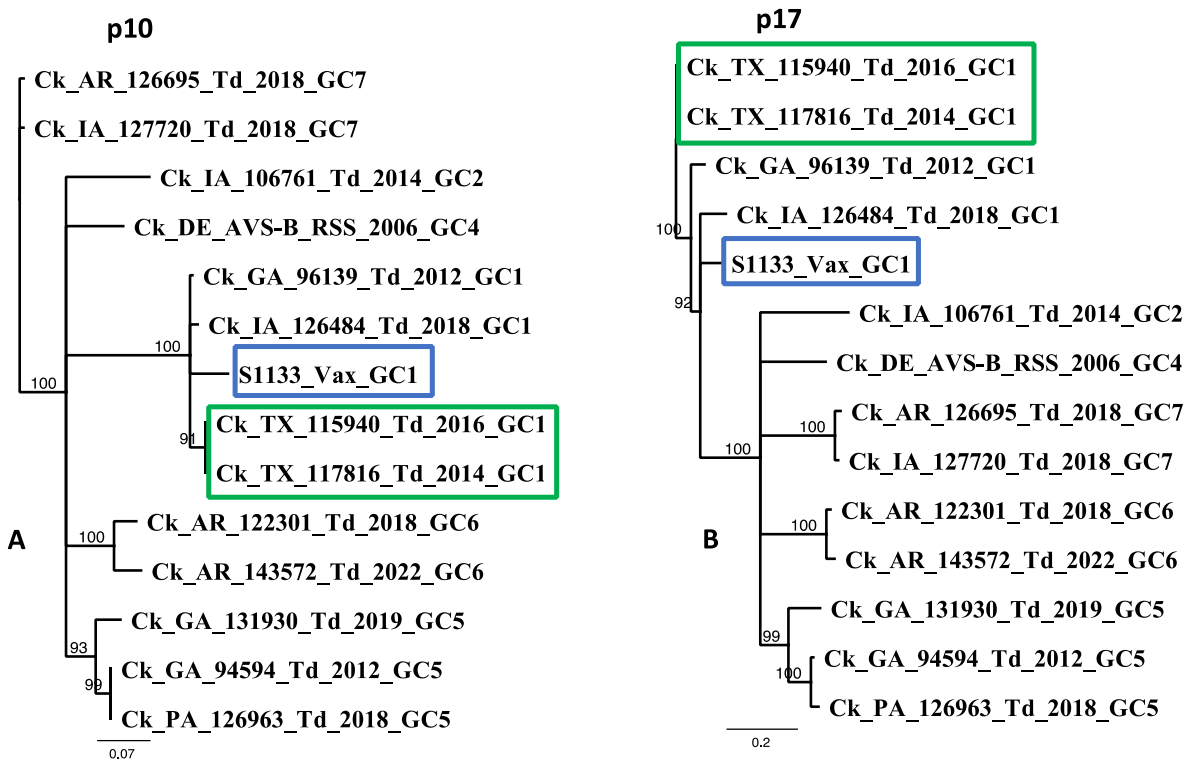

Fig. 4.4: Phylogenetic trees of ARV σC protein (A) and concatenated viral proteome (B). Field isolates sequenced in this study and strain AVS_B are named per convention proposed by Sellers, 2022 (3) and their specific GC is added to the end of their names. Green box delineates cluster that include GC1 variants 115940 and 117816 and blue box delineates S1133 vaccine strain.

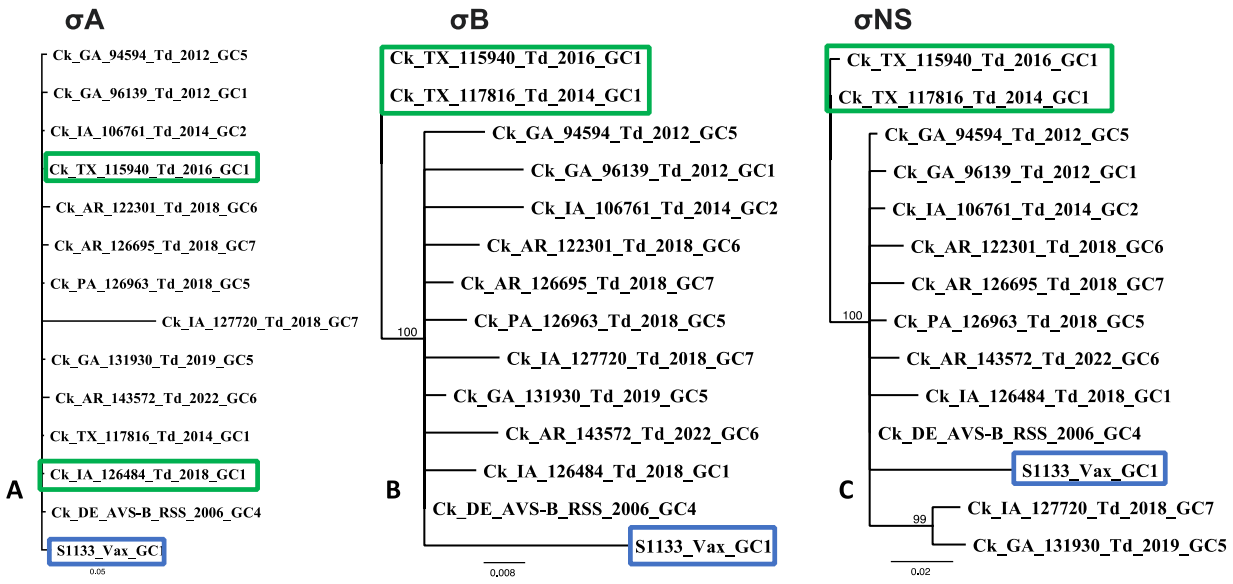

Fig. 4.5: Phylogenetic trees of σA (A), σB (B) and σNS (C) protein. Field isolates sequenced in this study and strain AVS_B are named per convention proposed by Sellers, 2022 (3) and their specific GC is added to the end of their names. Green box delineates cluster that include GC1 variants 115940 and 117816 and blue box delineates S1133 vaccine strain.

CHAPTER 5

DISCUSSION AND CONCLUSION

Poultry production is a cornerstone of both global economies and food security. In the United States, this industry drives over 500 billion USD in economic activity (1), while in developing countries, where it may be less impactful on the economy in monetary terms, it contributes immensely to food security and supply of animal protein.

The industry's staggering impact in the US was attainable by combining the various stages of production into large vertically integrated operations. These companies, through economies of scale and improved efficiency have vastly improved productivity at all levels in the industry's value chain. This, coupled with advancements in bird genetics, have helped to foster the affordability and appeal of poultry products. However, this highly integrated structure also amplifies the impact of outbreaks of new and emerging disease pathogens (2).

The transmission and persistence of pathogens such as avian reovirus (ARV) have been closely linked to practices common in highly efficient, vertically integrated operations. Practices including the mixing of eggs from multiple breeder flocks, short downtime in grow-out barns, and the maintenance of multi-age flocks in a single complex facilitate pathogen spread .ARV is the definitive cause of viral arthritis and tenosynovitis and has been isolated in several debilitating conditions of commercial poultry including myocarditis, enteritis, hepatitis, runting stunting (RSS) and malabsorption (MAS) syndromes (3-7). A trend emerged over a decade ago in which variant strains of ARV were increasingly being isolated from diseases of progeny of vaccinated flocks, and since that time it has become a source of significant economic loss to producers (8).

Structurally, ARVs are non-enveloped viruses possessing an icosahedral capsid with two concentric walls enhancing their stability in the environment (9). The viral genome consists of 10 segments of dsRNA molecules and are named based on their electrophoretic mobility, viz: large (L1-L3), medium (M1-M3) and small (S1-S4). This genome encodes 8 structural proteins (λA, λB, λC, μA, μB, σA, σB, and σC,) and 4 nonstructural proteins (μNS, σNS, p10 and p17) (10). The minor outer capsid protein - σC, mediates host cell attachment and is the target of neutralizing antibodies (11). Based on the sequences of the minor outer capsid protein - σC, 7 genotypic clusters have been identified to date (12).

Vaccination with modified live and killed vaccines remains a crucial tool for controlling this disease(11). However, increased variant isolation(12-18) suggests the waning efficacy of commercial vaccines, and a growing reliance on autogenous vaccines (8, 12). Therefore, the development of new broadly protective live attenuated and/or killed vaccine vaccines will be welcomed by the industry.

A pivotal step in the development of broadly protective vaccines is a thorough understanding of the spectrum of antigenic types circulating in the field. In addition, A persistent challenge in the molecular characterization of ARV is that the current typing system does not provide insights into the pathobiological properties of the isolates. An enhanced typing scheme that incorporates information on virulence, tissue tropism, and other characteristics relevant to ARVs pathogenicity would significantly improve the effectiveness of monitoring and surveillance efforts for this pathogen. A further complication in the characterization of ARV is the presence of multiple coinfecting strains within field isolates of the virus. Resolving this mixed ARV populations in field samples is important for accurately tracking ARVs across outbreaks and monitoring efficacy of control interventions. At the Poultry Diagnostic and Research Center

(PDRC), the workflow for resolving multiple ARV populations involves cloning of RT-PCR products into vectors and transforming chemically competent bacteria cells followed by sequencing of 5 clones. While this protocol is useful it is likely that the depth resolution achieved is limited since only minute subset of clones is sequenced.

To address these challenges, our project undertook three complementary studies. First, we conducted cross-virus neutralization assays using hyperimmune sera generated in specific pathogen-free chickens, revealing that each GC and subcluster likely represents a distinct serotype. Second, whole-genome sequencing of 12 ARV field isolates provided the first complete genome sequences of GC 7 isolates, and phylogenetic analysis showed all S1-encoded proteins viral protein and the entire viral proteome are largely congruent with the σC phylogeny. Third, the application of Oxford Nanopore Technologies MinION sequencing demonstrated superior resolution in identifying mixed ARV populations compared to traditional PCR cloning methods.

Together, these findings underscore the antigenic and molecular diversity, as well as the evolutionary dynamics of ARV. They also have important implications for vaccine development particularly the challenge of creating a broadly protective vaccine. As suggested by the study on serologic relatedness, this may be a more complex task than previously thought, thereby supporting vaccine strategies that prioritize multivalent formulations. Furthermore, the diversity of co-infecting ARV strains in field isolates appears broader than previously recognized when using conventional cloning and Sanger sequencing methods. Thus, highlighting the vast pool of viral genomes available for genetic reassortment and emergence of genetic variants.

Although this study was not primarily intended to define a new phylogenetic framework for ARVs, nonetheless, our analysis of ARV protein phylogeny revealed the diversifying influence of σC and other S1-encoded proteins. Consequently, we propose two possible approaches for

developing a new molecular typing scheme for ARVs: first, the σC protein may be indispensable for ARV phylogenetic analysis, as the phylogeny of the predicted whole proteome closely mirrored that of σC. Second, the strong phylogenetic influence of σC may mask the contribution of other proteins, suggesting that its exclusion or the use of a truncated version could allow additional viral proteins to more effectively shape ARV phylogeny.

References

1. French D. Incidence and economic impact of reovirus in the poultry industries in the United States. *Avian Diseases.* 66:432-434; 2022.

2. Crabb HK, Allen JL, Devlin JM, Firestone SM, Wilks CR, Gilkerson JR. Salmonella spp. transmission in a vertically integrated poultry operation: Clustering and diversity analysis using phenotyping (serotyping, phage typing) and genotyping (MLVA). *PLoS One.* 13:e0201031; 2018.

3. <Rosenberger et al.pdf>.

4. Rosenberger JK. Characterization of reoviruses associated with a runting syndrome in chickens. 1983 Sydney South 2000, Australia. Post-Graduate Committee in Veterinary Science, PO Box A561. p. 141-152.

5. Rosenberger JK. Role of avian reoviruses in malabsorption syndrome. *Proceedings of 32nd Western Poultry Disease Conference.*39-40; 1983.

6. Rosenberger JK, Olsen N, Van der Heide L. Viral arthritis/Tenosynovitis and other reovirus infections. *A laboratory manual for the isolation and identification of avian pathogens.* 4:207-210; 1998.

7. Jones RC. Avian reovirus infections. *Rev Sci Tech (International Office of Epizootics).* 19:614-625; 2000.

8. Sellers HS. Current limitations in control of viral arthritis and tenosynovitis caused by avian reoviruses in commercial poultry. *Vet Microbiol.* 206:152-156; 2017.

9. Savage CE, Jones R. The survival of avian reoviruses on materials associated with the poultry house environment. *Avian Pathology.* 32:417-423; 2003.

10. Benavente J, Martínez-Costas J. Avian reovirus: structure and biology. *Virus research.* 123:105-119; 2007.

11. Dawe W, Kapczynski D, Linnemann E, Gauthiersloan V, Sellers H. Analysis of the immune response and identification of antibody epitopes against the sigma C protein of avian orthoreovirus following immunization with live or inactivated vaccines. *Avian Diseases.* 66:465-478; 2022.

12. Sellers HS. Avian reoviruses from clinical cases of tenosynovitis: An overview of diagnostic approaches and 10-year review of isolations and genetic characterization. *Avian Diseases.* 66:420-426; 2022.

13. Ayalew LE, Ahmed KA, Mekuria ZH, Lockerbie B, Popowich S, Tikoo SK, Ojkic D, Gomis S. The dynamics of molecular evolution of emerging avian reoviruses through accumulation of point mutations and genetic re-assortment. *Virus Evol.* 6: English. 2020.

14. Egana-Labrin S, Hauck R, Figueroa A, Stoute S, Shivaprasad HL, Crispo M, Corsiglia C, Zhou H, Kern C, Crossley B*, et al.* Genotypic Characterization of Emerging Avian Reovirus Genetic Variants in California. *Sci Rep-Uk.* 9: English. 2019.

15. Goldenberg D, Pasmanik-Chor M, Pirak M, Kass N, Lublin A, Yeheskel A, Heller D, Pitcovski J. Genetic and antigenic characterization of sigma C protein from avian reovirus. *Avian Pathol.* 39:189-99; 2010.

16. Kant A, Balk F, Born L, Van Roozelaar D, Heijmans J, Gielkens A, Ter Huurne A. Classification of Dutch and German avian reoviruses by sequencing the sigma-C protein. *Veterinary research.* 34:203-212; 2003.

17. Nour I, Alvarez-Narvaez S, Harrell TL, Conrad SJ, Mohanty SK. Whole genomic constellation of avian reovirus strains isolated from broilers with arthritis in North Carolina, USA. *Viruses.* 15:2191; 2023.

18. Troxler S, Rigomier P, Bilic I, Liebhart D, Prokofieva I, Robineau B, Hess M. Identification of a new reovirus causing substantial losses in broiler production in France, despite routine vaccination of breeders. *Veterinary Record.* 172:556; 2013.